POLITEKNIK NEGERI BALI

Journal of Engineering Design and Technology

logic

Vol. 24 No. 1 March 2024

LOGIC

Jurnal Rancang Bangun dan Teknologi

p-ISSN. 1412-114X

e-ISSN. 2580-5649

LOGIC

Jurnal Rancang Bangun dan Teknologi

Journal of Engineering Design and Technology

Gedung P3M, lt.1 Politeknik Negeri Bali, Bukit Jimbaran
PO BOX 1064 Kuta Selatan, Badung, Bali - Indonesia
Telp. (+62)361 701981 Fax. (+62)361 701128
Email: logic@pnb.ac.id

LOGIC JOURNAL TEAM

PREFACE

Logic: Jurnal Rancang Bangun dan Teknologi (Journal of Engineering Design and Technology) is a peer-reviewed research journal aiming at promoting and publishing original high quality research in all disciplines of engineering and applied technology. All research articles submitted to Logic should be original in nature, never previously published in any journal or presented in a conference or undergoing such process across the world. All the submissions will be peer-reviewed by the panel of experts associated with particular field. Submitted papers should meet the internationally accepted criteria and manuscripts should follow the style of the journal for the purpose of both reviewing and editing.

Logic is a journal covering articles in the field of civil and mechanical engineering, design, and technology published 3 times a year in March, July, and November. Language used in this journal is English.

LOGIC. P-ISSN 1412-114X
LOGIC. E-ISSN 2580-5649
Indexing : GOOGLE SCHOLAR, DOAJ, EBSCO OPEN SCIENCE DIRECTORY, SINTA, GARUDA

Best Regard,

LOGIC Editorial Team

TABLE OF CONTENTS

LOGIC
Journal of Engineering Design and Technology
Vol. 24 No.1 March 2024 ; p. 1 - 8

p-ISSN : 1412-114X
e-ISSN : 2580-5649
http://ojs2.pnb.ac.id/index.php/LOGIC

DESIGN OF MULTIFUNCTIONAL MANUAL SCREEN PRINTING TOOL

I Nengah Ludra Antara[1*)], I Nyoman Sutarna[2)], I Putu Darmawa[3)], I Nyoman Gunung[4)]

1,2,3,4) Mechanical Engineering, Politeknik Negeri Bali, Denpasar, Indonesia

Correponding email [1*)]: nengahludraantara@pnb.ac.id

Abstract. Screen printing is the simplest and most likely done manually. This screen printing technique is also an effective and efficient way to develop small industries. The advantage of this screen printing business is that the capital is not too large, and you also don't have to have special skills. This research method is to redesign the manual screen printing tool by combining two screen printing tools to get more effective and efficient results for the screen printing operator. The research results show that the advantage of redesigning this screen printing tool is that it can produce precise print results and can print several screen-printed objects that previously could only produce plastic screen prints. After adding a design, the function of the tool will increase to be able to filter glass, cardboard, plastic bags, etc.

Keywords: screen printing, stickers, cup molding, multifunction.

1. INTRODUCTION

Along with the growth of the screen printing business, stickers, plastic and glass screen printing have become a necessity for entrepreneurs so that the brand or identity of a beverage and convection product can be recognized by people. Therefore, screen printing stickers, plastic and glass are in great demand for entrepreneurs who want to market their products in a wider range. According to my survey, the author did in Gianyar Regency, Singapadu Village, there are many convection businesses and sales of boba drinks. So it requires a fast printing process. The existing screen printing process in Singapadu Village uses a separate screen printing tool in the sense that the sticker and plastic bottle screen printing tools are separate, so it takes a relatively long time. In addition, screen printers also feel uncomfortable. As the times progress, there are various types of tools that can simplify the screen printing process. Because the existing screen printing tools at Delivery Konveksi are less efficient due to the limitations of the print media. Therefore, in order to compete with screen printing tools that are still very expensive on the market, we have an initiative and an idea to design a multifunctional manual screen printing tool so that the middle class can open a business with limited capital. So that the thought arose to design a tool, namely the design of a multifunctional manual screen printing tool, and the author hopes that with this tool, it can help the screen printing business in the process of printing. And more economical so that it can be reached by convection and young people who start a screen printing business in Singapadu Village.

Design is the engineering of a construction or structure that realizes the concept of being an item or tool [1], [2]. The activity of planning or designing a construction must consider the following criteria, easy and simple, easy to make or common components on the market, economical is a service that has the best quality at the smallest possible price level and aesthetic is a sense that arises from how beautiful or dazzling an object is seen and the tool must be aesthetic in shape and appearance, and appropriate in a technology that is discovered or created with the aim of further improving or making human work smoother. This can then increase economic value as well, the technology is not just made but made precisely according to human needs [3]–[5].

Manual Screen Printing Tools The word screen printing comes from the Dutch language, namely "scablon", in the language of absorption into screen printing. Screen printing is part of the science of applied graphics that is practical. Screen printing is the simplest print and is likely to be done manually. This printing technique is also an effective and efficient way of developing small industries. The advantage of this screen printing business is that the capital is not too large, and also does not have to have special skills. With willingness and practice, anyone will be able to do this job. Furthermore, with perseverance and good processing, it will

produce good results, so many people make screen printing tools with limited use of screen printing media on their own. The idea of redesigning my manual screen printing tool came from problems at Delivory Konveksi. The purpose of designing this screen printing tool is to add 1 cup bottle screen printing tool to get more effective and efficient results.

Screen printing screen is an item that is needed as one of the equipment for screen printing [6]. There are two parts to the screen printing screen, namely the main part, namely the frame and the screen cloth or gauze. Where the frame used on the screen printing screen can be made of aluminum or wood. The frame functions to give shape and hold the screen printing ink to stay on the screen printing field [7]. Screen printing frames are usually made in various sizes, adjusted of course to the needs of the screen printing to be carried out (the size of the image to be screened). Screen printing frame materials can be made of wood, aluminum, or sometimes also hollow iron [8].

Based on the design and purpose of using the screen. screens that are generally used to make screen printing on fabric as a whole can be divided into several categories [9], [10]. Namely starting from a coarse screen (48 T-90 T), medium screen (120 T-150 T), to a fine screen (165 T-200 T). The letter T listed in front of the number is usually termed Thick which is then abbreviated as T. The size of T in the screen printing world is commonly used to indicate the level of density in the woven screen threads [11]. The bigger the number, the tighter the yarn.

In the design of a multifunctional manual screen printing tool, the author only discusses how to design/make a multifunctional manual screen printing tool. In this design, the author uses problem boundaries so that the discussion does not get out of the existing objectives. The problem limitation used is how to design or make a multifunctional manual screen printing tool and the community easily uses the designed tool so that it can increase productivity for convection and screen printing workers. Increasing worker productivity is very necessary for small and medium industries [12], [13].

The objectives of the research of the design of a multifunctional manual screen printing tool are: 1) To find out how to design or make a multifunctional manual screen printing tool, 2) With the design of this multifunctional manual screen printing tool, it can increase productivity for convection and screen printing workers.

2. METHODS

The type of research taken uses the type of design research. Design is planning, designing, engineering calculations of materials and components, simulation tests, and modeling of a tool [14], [15]. In the design the author took the title "Design of Multifunctional Manual Screen Printing Tools". The completion of this design uses an exploratory method that aims to find a new solution to solve the problems faced by convection and screen printers. The first step in this exploratory research is to add a cup bottle screen printing tool that once screen printing gets a lot of screened cup bottles faced by screen printers, by conducting a survey in the field. After obtaining the required data then design, calculate, select the materials to be used. And solve existing problems by realizing a design [16].

Figure 1. Plastic screen printing tools

Employees who work in screen printing or convection, located in Singapadu Banjar Negari Village, Sukawati District, Gianyar Regency, Bali Province, as in Figure 1, still use simple tools in doing a job of printing plastic, stickers, shopping bags by using separate tools, causing the production process to be longer and the area used is more.

In every design, of course, there are pictures of components and their arrangement so that later it will make it easier when working or realizing the design made, as well as in the design of this multifunctional manual screen printing tool. In designing images using the *Professional Autodesk Program Inventor Drawing Des*ign *2018*. As in Figure 2.

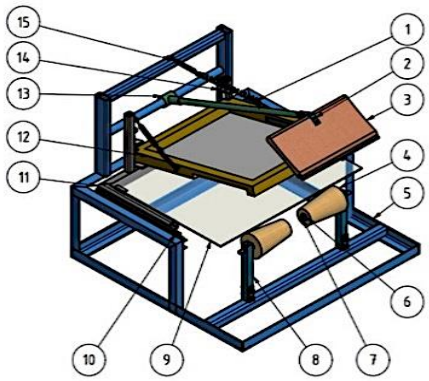

1.Gas spiral
2.Bolt
3.Rackel
4.Molding cup
5. Frame
6. Bearing
7.Nut
8.Molding cup handle
9. Glass
10. Drawer rail low profile opening ¾
11. Screen printing frame of glass and screen
12. Screen molding cup
13. Screen printing rod
14. Screen sheet clamp
15.Turnbuckle

Figure 2. Design Of Multifunctional Manual Screen Printing Tool

Some of the tools and materials used in this study, namely:

2.1 Tools

To support the work of "Design of Multifunctional Manual Screen Printing Tools", using some of the following equipment: Welding machine, hand grinder, compressor, drilling machine, lathe, vernier, steel bar, and elbow.

2.2 Materials

To realize the process of multifunctional manual screen printing tools, the following materials are needed:

Table 1. Materials

No	Component name	Quantity (pieces/cm)
1	Rackel	1
2	Screen and frame	30cm x 40cm
3	Glass	30cm x 50cm
4	Moulding cup	2
5	Screen sheet clamp	2
6	Drawer rail low profile opening ¾	2
7	Spiral spring	2
8	Turnbuckle	2
9	Spiral spring	3cm x 3cm
10	Iron pipe	Ø 8mm
11	Bolts and nuts	10
12	Hollow iron	3cm x 3cm
13	Bearings	4

.

The procedure research with the following stages :

1) Conducting observations or research in the field to find problems in the field so that later the tool can be appropriate.
2) Determining the needs of the tool to determine the concept of the tool so that it is effective and efficient.
3) Making drawings or designs to determine the shape and mechanism of the sketch design of the tool to be made.
4) Determining the cost details needed to make the tool to be made.
5) The process of making or working on tools according to the working drawings.
6) The process of assembling, finishing and testing the results of the design.

3. RESULTS AND DISCUSSION

3.1 Design Results

The resulting design is as follows.

Figure 3. Multifunctional manual screen printing tool

Deck 1, flat surface screen printing (paper bag and sticker screen printing)

a) Prepare tools and materials before performing the screen printing process.
b) Install the glass mat for the placement of the product to be screened.
c) Place the screen above the product to be screened.
d) Setting the distance of the rackel from the screen.
e) Pour screen printing paint into the screen and mix a little with m4.
f) Rub the screen that has been painted using the racket.
g) Lift the screen and replace the product, do it repeatedly.

Deck 2, screen printing the surface of round objects or tubes (cup screen printing)

a) Prepare tools and materials before the screen printing process.
b) Remove the glass mat.
c) Install the screen on the sliding track.
d) Setting the racket and the position of the holder for the product.
e) Pour the screen printing paint into the screen.
f) Slide the screen back and forth with the handle.
g) Lift the screen and replace the product, do it repeatedly

3.2 Materials used

The materials used in this design are shown in Table 2.

Table 2. Materials Description

Name	Specification	Quantity	Description
Hollow Iron	3mm x 3mm	1 pc	made
Iron plate	3mm	1 pc	made
Iron pipe	O 1- inch	1 pc	made
Angle iron	3mm x 3mm	1 pc	made
Rackel	wood and rubber	2 pcs	bought
Screen	30 cm x 40 cm	2 pcs	bought
Glass	40cm x 50 cm	1 pc	bought
Turnbuckle	stainless	2 pcs	bought
Spiral spring	steel wire	2 pcs	bought
Low profile drawer rails	opening ¾	2 pcs	bought
Moulding cup	wood	2 pcs	bought
Screen clamp	steel	2 pcs	bought
Bolts and nuts	steel	8 pcs	bought
Couplers	steel	8 pcs	bought
Bearings	steel	4 pcs	bought

3.3 Manufacturing Process of Multifunctional Manual Screen Printing Tool Frame

The process for making a multifunctional manual screen printing tool frame is as follows.

Figure 4. Welding process

Figure 5. Smoothing process

3.3.1 Cup molding process

1) Tools used: lathe (wood chisel), wedge, sandpaper.
2) Materials used: panis wood
3) Working process
    a) Pay attention to the work drawings carefully.
    b) Prepare the tools and materials used.
    c) Take measurements and markings according to the working drawings, after that just do the turning on the material that has been marked.
    d) After molding the cup according to the size or working drawing, then make a hole in the center of the molding cup for the bearing and shaft so that it can rotate.
    e) After finishing turning and making holes then smooth the molding cup with sandpaper to make it smooth.
    f) Finish the new smoothness to do the painting process.

Figure 6. Turning process

3.3.2 Painting Process

The painting process uses the following tools and materials

1) Tools used: 280 grit sandpaper and 800 grit putty, kapi
2) Materials used:
3) The steps of caulking process on the frame
   a) Leveling the uneven surface of the iron and smoothing the welding marks.
   b) The process of caulking on the frame is carried out to flatten the welding connection and flatten the surface of the iron that is accidentally exposed to burrs.
   c) Then smooth the parts that have been putty with 280 grit sandpaper and 800 grit.

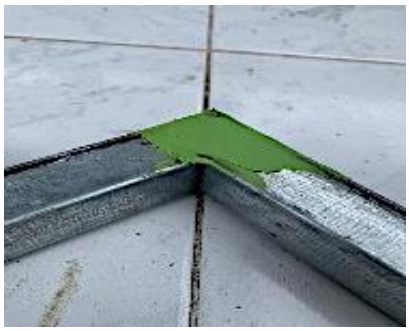

Figure 7 Putty process

4) Painting process with primer (*epoxy*)
   a) Sand the iron surface using 200 grit sandpaper.
   b) Wash with soap until clean.
   c) Wipe and dry until the frame, glass holder and molding cup holder are completely dry.
   d) dry completely.
   e) Epoxy all parts of the frame, glass holder and molding cup holder. Repeat 2x basic bonding (epoxy).

Figure 8 Primer

5) Painting process with blue paint
   a) Sand the surface that has been epoxied with 800 sandpaper.
   b) Wash with soap until clean.
   c) Wipe and dry until the frame, glass holder and molding cup holder dry completely.
   d) Paint using blue sapire colored paint to all parts of the frame.

Figure 9 Blue color painting

3.4 Testing Process

Based on the results of tests carried out 5 times on (deck 1, flat screen printing for sticker, paper bag, and plastic screen printing) and tests carried out 10 times on (deck 2, surface screen printing of round objects or tubes for cup screen printing). Observation data was obtained in the form of a comparison of the use of ordinary screen printing tools with multifunctional manual screen printing tools. Based on the data analysis carried out, the advantages and disadvantages of multifunctional manual screen printing tools are obtained as in Table 3.

Table 3. Test Results

Parameter	Sticker screen printing tools and paper bag	Cup screen printing tool	Manual screen printing tool multifunction
Screen printing result	Less neat, because it is not equipped with a sturdy frame and it takes time to position and lock the object to be screened.	Expression is difficult to achieve, needs to be set up and tested before use.	Precision, because the frame is made strong to keep the object being screened from moving (Deck 1, flat surface screen printing for sticker, paper bag, plastic screen printing) and the screen printing point according to the design is not tilted or defective. (Deck 2, surface screen printing of round objects or tubes for cup screen printing)
Usage	Long process, need time to set the tool for precision screen printing results with the object.	Long process, cannot screen print quickly and neatly, slippery cup holder cannot lock well. lock well.	Practical, and easy to operate according to the object to be screened.
Operator	1 operator, to screen 1 type of object.	1 operator, for printing 1 type of object.	1 operator with dual-function tools.
Place	A table is required for the work process because the object being screened must be on a flat surface.	A table is required for the work process due to the small size of the tool.	Minimalist in shape, it takes up little space and does not require a table.

4. CONCLUSION

Based on the results of the trial use of a multifunctional manual screen printing tool, a significant difference was obtained compared to the usual tool. In terms of cost, time and workplace requirements. In terms of cost, the multifunctional manual screen printing tool can cut operator costs and tool procurement costs, while in time the multifunctional manual screen printing tool is easier to operate and more efficient because of its multifunctional features, while from the needs of the production site the multifunctional manual screen printing tool is more compact and takes up less space.

The screen printing results obtained by the multi-function manual screen printing tool are considered more precise because the frame and body of the tool are strong to maintain the stability of the object when screened, especially when the cup screen printing process. The operator required to operate the tool is only 1 person with experience and skills in printing plastic and cup screen printing. Some of the advantages of multifunctional manual screen printing tools:

1) This tool can screen different objects with 1 tool.
2) This tool is easy to operate because it is only set once.
3) The shape of the tool is easy to move.

4) The cost of the tool is cheaper than before.
5) To increase the life of the tool, periodic maintenance should be carried out and after use is always cleaned.
6) In the design of this multifunctional manual screen printing tool there are still many shortcomings, therefore it is hoped that in the future this tool can be analyzed and redesigned (redesign) so that it can be developed for its improvement.

5. REFERENCES

[1] P. L. Dhar, "Chapter 7 - Introduction to Optimum Design," P. L. B. T.-T. S. D. and S. Dhar, Ed. Academic Press, 2017, pp. 385–407.
[2] J. Wickert and K. E. Lewis, *Mechanical Engineering, An Introduction to Mechanical Engineering*, Third Edit. Canada: Nelson Education Ltd., 2013.
[3] A. Parrish and F. J. Camm, *Mechanical engineer's reference book*, 11th Editi. London: Butterworths, 2011.
[4] B. Kaur, "A Study : Working Conditions Of Small Scale Weaving Units," *Int. J. Mech. Eng.*, vol. 7, no. 1, pp. 1375–1379, 2022.
[5] I. G. Santosa and M. Yusuf, "Ergonomic Multifunctional Building Tool Design to Increase Work Productivity of Msmes Employees," *Am. J. Sci. Eng. Technol.*, vol. 8, no. 4, pp. 189–193, Oct. 2023.
[6] J. Cao, "Research on the Fusion of Art Design and Screen Printing Process," in *Proceedings of the 2021 Conference on Art and Design: Inheritance and Innovation (ADII 2021)*, 2022, vol. 643, no. Adii 2021, pp. 311–316.
[7] K. Dölle, "Original Research Article Paper for Screen Printing Applications – A Paper Development Study," *J. Eng. Res. Reports*, vol. 21, no. 9 SE-Original Research Article, pp. 45–63, Dec. 2021.
[8] V. Cazac, J. Cîrja, E. Balan, and C. Mohora, "The study of the screen printing quality depending on the surface to be printed," *MATEC Web Conf.*, vol. 178, pp. 1–6, 2018.
[9] J. Lavanya and N. Kishore, "Different Textile Printing Techniques-Hand Block Printing, Screen Printing, And Digital Printing," *Webology*, vol. 19, no. 2, pp. 787–802, 2022.
[10] U. Boda, J. Strandberg, J. Eriksson, X. Liu, V. Beni, and K. Tybrandt, "Screen-Printed Corrosion-Resistant and Long-Term Stable Stretchable Electronics Based on AgAu Microflake Conductors," *ACS Appl. Mater. Interfaces*, vol. 15, no. 9, pp. 12372–12382, Mar. 2023.
[11] U. Hasni, M. E. Piper, J. Lundquist, and E. Topsakal, "Screen-Printed Fabric Antennas for Wearable Applications," *IEEE Open J. Antennas Propag.*, vol. 2, pp. 591–598, 2021.
[12] M. Yusuf, L. Sudiajeng, K. A. Suryawan, and I. M. Sudana, "Redesign of Ergonomic Worktables in Reinforced Concrete Sheet Works Reduce Ergonomic Risk Level," in *Proceedings of the 5th International Conference on Applied Science and Technology on Engineering Science iCAST-ES*, 2022, pp. 370–374.
[13] T. Budiyanto and M. Yusuf, "Improvement of Wok Molding Station Increases Work Comfort and Productivity of the Workers," *Int. J. Psychosoc. Rehabil.*, vol. 24, no. 4, pp. 8883–8892, 2020.
[14] C. Qiu, J. Tan, Z. Liu, H. Mao, and W. Hu, "Design Theory and Method of Complex Products: A Review," *Chinese J. Mech. Eng.*, vol. 35, no. 1, p. 103, 2022.
[15] D. Mourtzis, "Simulation in the design and operation of manufacturing systems: state of the art and new trends," *Int. J. Prod. Res.*, vol. 58, no. 7, pp. 1927–1949, Apr. 2020.
[16] I. G. O. Pujihadi, I. K. G. J. Suarbawa, I. M. Arsawan, and M. Yusuf, "Coffee Roasting Machine Model Design 3Kg Capacity to Boost Craftsman Work Productivity," *Am. J. Appl. Sci. Res.*, vol. 8, no. 4, pp. 83–87, 2022.

LOGIC
Journal of Engineering Design and Technology
Vol. 24 No.1 March 2024 ; p. 9 - 16

p-ISSN : 1412-114X
e-ISSN : 2580-5649
http://ojs2.pnb.ac.id/index.php/LOGIC

THE EFFECT OF THE ANGLE AND DIMENSIONS OF A CROSS-SECTION SPECIMEN ON THE TORSIONAL STRENGTH OF AISI 1020 SQUARE STEEL SHAFT

Bima Cahya Maula Dana [1)], Syamsul Hadi [2)], Hangga Wicaksono [3)], Kris Witono [4)]

1,2,3,4) Mechanical Engineering Department, State Polytechnic of Malang, Jl. Soekarno-Hatta 9, Malang, Indonesia

Correponding email [2)] : syampol2003@yahoo.com or syamsul.hadi@polinema.ac.id

Abstract. The unknown torsional strength due to the inconsistency of the angles and dimensions of the square cross-section of AISI 1020 steel specimens in the torsion test is the problem encountered. The research method included: preparation of square AISI 1020 steel specimens measuring 6 mm x 6 mm x 160 mm, measurement of 2 diagonal angles of the cross section of the specimen and dimensions of the cross section at 5 observation points along the specimen receiving torsion loads, torsion testing of specimens, analysis of torsion test results data, and drawing conclusions. The results of the study affect the angle and dimensions of the specimen cross-section on the torsional strength of the AISI 1020 steel square shaft which has a greater value at the angles of 89° and 91° than 90° which with an angle of 89° at dimensions of 5.96 mm x 5.96 mm has a torsional strength of 412 MPa, while at an angle of 90° with dimensions of 5.96 mm x 5.96 mm it has a torsional strength of 359 MPa, and for an angle of 91° in dimensions of 5.95 mm x 5.95 mm has a torsional strength of 402 MPa. The average torsional strength is achieved in the range of 351 to 397 MPa, at an angle of 89° the torsional strength increases by 46 MPa or around 13.1 %, and at an angle of 91° the torsional strength increases by 43 MPa or around 12.3%.

Keywords: Specimen cross-sectional angle, Specimen cross-sectional dimensions, AISI 1020 steel, square shaft, Torsional strength.

1. INTRODUCTION

Improvement of material toughness due to hardening and tempering has been carried out on low carbon steel with pressurized water, air and oil [1]. By heat treatment the toughness of low carbon materials can be increased. Fabrication of metal materials for the industrial world is carried out by forging, rolling and extruding in which rolling is carried out by clamping the plate between two rollers from the pressure roller and the main roller which rotates in opposite directions, so that it can move the plate [2]. In rolling it cannot be guaranteed to produce a cross section that is truly 90° angled with uniform rectangular dimensions. The rotary bending test obtained the maximum safe limit value for the torsional stress of 283.95 MPa which meets the requirements for ship shaft materials [3]. It is important to know the torsional strength of the shaft prior to use so as not to exceed the specified allowable value. Research on hardened S45C steel showed that the torsional strength was 425.67 MPa with the dominant ferrite phase microstructure and the tempering results were 392.7 MPa lower with the dominant pearlite phase microstructure [4]. Shaft heat treatment provides increased torsional strength. The results showed that ST 60 steel for the propeller shaft with hardening heat treatment followed by tempering had a torsional strength of 737.72 MPa [5]. ST 60 steel has higher torsional strength than S45C steel. Coating material that is softer or less rigid than the shaft material can reduce the maximum value of the stress on the shaft cross section [6]. The softer nature of the coating material contributes to lowering the stress on the shaft being coated. The torsional moment of ST 37 is lower than that of ST 90, then the torsional moment of ST90 is lower than that of VCN [7].

The torsional moment reflects the torsional strength of the material being tested for torsion. Low carbon steels produced in the largest quantities are included in the low carbon classification which generally contain less than 0.25% by weight C and are unresponsive to heat treatment intended to form martensite, reinforcement is done by cold working. The microstructure consists of the constituents ferrite and pearlite which as a result, the alloy is relatively soft and weak, but has outstanding ductility and toughness [8]. Low carbon steels are very ductile and cannot be heat treated, except hardened by carburizing. The increase in stiffness in torsion of a flat bar is highly dependent on the width and thickness of the flat bar, separation/expansion distance, and angle of twist. The torque angle resulting from the bonded bending of 2 plates whose ends are welded for a length of 528 mm, a width of 30 mm to 60 mm for a thickness of 3 mm and 6 mm achieves a total torque of around 5.3% to 10.1% [9]. Twisting of flat reinforcement is affected by its dimensions, separation distance and angle of twist. The GGM 90 W motor type in the torsion testing machine modification has a torque of 408.9 Nmm and a rotation output of 124 rpm [10]. The speed of the manual motor drive modification is relatively unstable compared to the drive using an electric motor in a torsion testing machine with a constant rotation.

The results showed that ST 41 steel with quenching heat treatment had a torsional strength of 448.65 MPa [11]. Medium carbon steel can be heat treated, so that the strength can be increased after heat treatment. The results of the ABS, PET and PLA torsion tests showed that the highest torque of acrylonitrile butadiide styrene (ABS) was achieved at 230 ^{o}C compared to 240 ^{o}C, 250 ^{o}C and 260 ^{o}C; for PET material, the highest torque is achieved at a temperature of 235 ^{o}C compared to temperatures of 220 ^{o}C, 230 ^{o}C and 240 ^{o}C; and for polylactic acid (PLA) materials the highest torque is achieved at a temperature of 215 ^{o}C compared to temperatures of 200 ^{o}C, 205 ^{o}C and 210 ^{o}C [12]. The molding temperature of ABS, PET and PLA materials affects the torque or torsional strength of the plastic material. One of the main problems in the design of machine components that receive torsional stresses is determining the optimal shape and dimensions so that they can withstand the torsional loads they receive [13]. Optimal design of a component can save costs, volume of materials and duration of the processing process.

The results of the geometry and modeling of the torsion test specimen according to ASTM E-143 show that the stress distribution that occurs on the surface area of the specimen is not significant between 2.879e+09 Pa and 2.973e+09 Pa [14]. The stress distribution that occurs on the surface of the specimen area is influenced by the geometry and modeling designed in the simulation. The standard test equipment has maximum strength when the specimen breaks at an angle of 130^{o} third round with a torsional moment of 3.37 Nm, and the design test equipment has maximum strength when it breaks at 230^{o} fourth round with a torque reading of 3.65 Nm. The maximum torsional strength is a difference of 7.67% from 3.65 Nm [15]. If there is a difference in the torsional strength results between the manual torsion testing machine and the electric motor drive, it is necessary to adjust the length of the arm and calibrate it. The results of the three-point bending test and torsion test show that the stress distribution on the rectangular hollow cross-section (RHS) shows that the use of direct-forming with welding of edge (DFW-RHS) as a reinforcing beam has higher stiffness compared to direct-forming (DF-RHS), which means that under identical loading, direct forming (DF-RHS) with t = 1.93 mm has the same stiffness as direct forming with edge welding (DFW-RHS) with t = 0.7 mm, that is, the potential for reducing metal materials is 62% [16]. With a special shape profile that increases stiffness can save the use of materials to obtain the same stiffness value.

2. METHODS

Torsion test on a specimen is carried out to determine the plasticity of a material. The specimens used in the torsion test are rods with circular/square cross-sections for the simplest cross-sectional shapes, so they are easy to measure. The specimen is only subjected to a twisting load at one of the two ends. With torsional loading the specimen is forced to twist until it breaks, the recorded torsional force value is calculated to be the torsional moment and the twist angle value is used to plot the twisting performance curve. From the torsional moment, the torsional stress acting on the specimen can be calculated. The existence of specimens in the torsion test was chosen as a square shape which is not guaranteed to have an exact 90^{o} angle and the dimensions along the torsion area are also not guaranteed to be uniform, therefore in this study it was observed to analyze its effect on the torsional stress that occurs. The measurement of the right angle was carried out in a diagonal position with 5 (five) times replication along the torsion area and similarly for non-uniformity of the dimensions of the height and width of the cross-section was measured with 5 (five) times of replication as well.

In the plastic region, the relationship between the torsional moment and the torsion angle is non-linear, the shear stress can be calculated using Formula (1) [11].

$$\tau = \frac{T.c}{J} \quad (1)$$

Where T: torsion moment measured during torsion test, T = force x torsion arm = F. l; c: distance to the outermost fiber for a square cross section or the radius of a circle for a cylindrical cross section.
Polar moment of inertia for cylindrical, square and triangular cross sections [12].

$J = \pi D^4/32$ for the cylindrical cross section (2)

$J = (bh^3+b^3h)/12$ for square cross section (3)

$J = (bh^3+hb^3)/12$ for triangular cross section (4)

Shear Elastic Modulus, G:

$G = \tau / \gamma = T.L/J.\ \theta$ (5)

Where: τ: shear stress; γ: shear strain; T: torsional moment (torque); L: length of shaft subjected to twist; J: polar moment of inertia; and θ: the angle of internal twist (the circumference of a circle is 360° or 2π, with units conversion 360/2π = 360 x 3.14 = 57.3 in degrees = 1 radians) is shown in Equation (5).

The specimens used for testing are low carbon steel types following the ASTM (American Society of Testing and Materials) standard type E-143-02 Standard Test Method for Shear Modulus at Room Temperatures is shown in Figure 1 and Table 1 [17].

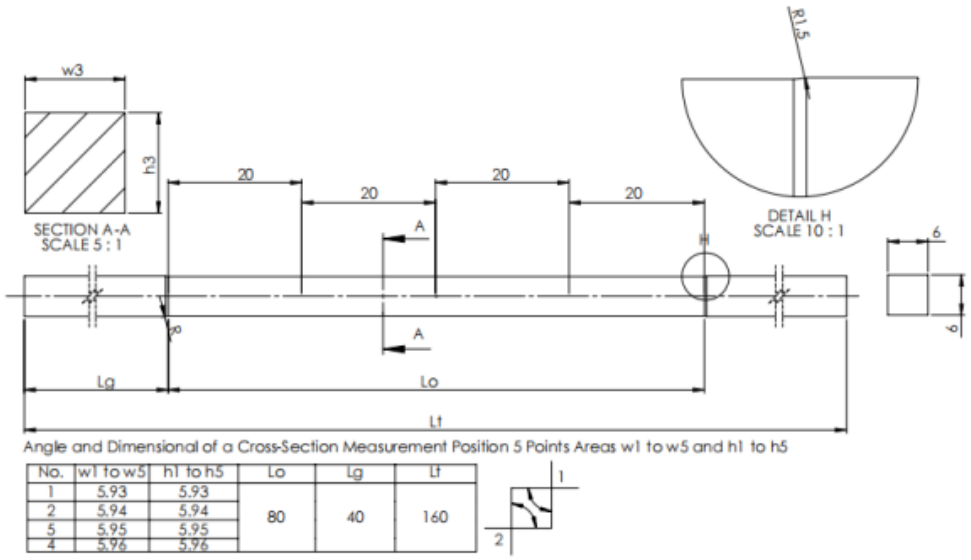

Figure 1. The shape of the torsion test specimen [17]

Table 1. Twist Test Specimens

Test Specimens	Specimen Dimensions (mm)					
	Do	Lo	R	Dg	Lg	Lt
ASTM E143-13	5.93, 5.94, 5.95 dan 5.96	80	1.5	6.64	39	160

The AISI 1020 steel selected for the study contains 0.20% carbon which can be designated as low carbon steel and its chemical composition is shown in Table 2.

Table 2. Chemical Composition of AISI 1020 Steel

No.	Element	Content (wt%)
1	Carbon (C)	0.142
2	Silicon (Si)	0.210
3	Manganese (Mn)	0.551
4	Phosphorous (P)	< 0.0100
5	Sulphur (S)	0.027
6	Chromium (Cr)	0.028
7	Nickel (Ni)	0.061
8	Molybdenum (Mo)	0.010
9	Copper (Cu)	0.093
10	Aluminium (Al)	< 0.0050
11	Titanium (Ti)	0.0030
12	Ferro (Fe)	98.85

Specifications for torsional test specimens made of AISI 1020 steel with dimensions of 6 mm x 6 mm x 160 mm with mechanical properties is shown in Table 3. The test is carried out with 4 sizes in the range from minimum to maximum of 5.93, 5.94, 5.95, and 5.96 mm with angles of 89°, 90° and 91° with 3 replications, so that the number of torsion test specimens is thirty-six.

Table 3. Mechanical Properties

Property	Tensile Strength	Yield Strength	Modulus of elasticity	Poisson ratio	Elongation at Break	Hardness
Metric	420 MPa	350 MPa	186 GPa	0.29	15%	110-121 BHN

Arrangement of research equipment was carried out with the following procedures: (1) cutting of low carbon steel AISI 1020 in a square shape measuring 6 mm x 6 mm x 160 mm in a total of thirty six specimens; (2) cleaning the specimen from dust, rust and checking its alignment; (3) marking a distance of 20 mm for 5 points in the torsion area, (4) measuring the dimensions (height and width) of the section using a vernier caliper, (5) measuring at 2 angles with the bevel protractor at the diagonal position of the section at 5 marked points; (6) recording the results of measurement of dimensions and angles into the specimen data sheet; (7) setting the torsion testing machine by adjusting the length of the specimen to 160 mm by installing 2 auxiliary tools in the form of 3 legs with a square hole measuring 6 mm x 6 mm which can be entered at both ends of the specimen to ensure that slippage cannot occur when the specimen is twisted, and (8) clamping the two ends of the specimen to a depth of 20 mm from both ends by tightening the two chucks contained in the torsion testing machine scheme is shown in Figure 2.

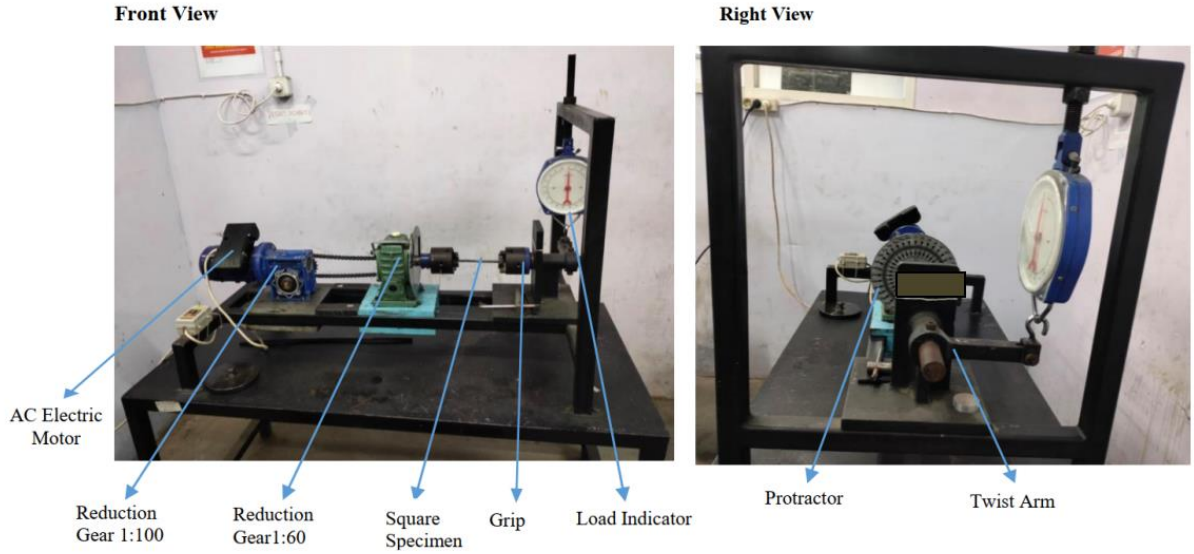

Figure 2. Schematic of torsion testing of square specimens

3. RESULTS AND DISCUSSION

The specimen before the torsion test is shown in Figure 3 and the specimen after the torsion test is shown in Figure 4.

Figure 3. Torsion test specimens before testing

Figure 4. Torsion test specimens after testing

Table 4. The torsional strength results from square shaft torsion tests

Specimen cross-sectional angle (°)	Specimen cross-sectional dimensions (mm)	Torsional strength (MPa)		
		Replication		
		1	2	3
Angle 89°	5.93 x 5.93	394	395	382
	5.94 x 5.94	403	380	405
	5.95 x 5.95	380	401	414
	5.96 x 5.96	387	412	412
Angle 90°	5.93 x 5.93	354	354	344
	5.94 x 5.94	331	343	364
	5.95 x 5.95	330	351	330
	5.96 x 5.96	329	359	350
Angle 91°	5.93 x 5.93	405	395	405
	5.94 x 5.94	381	405	393
	5.95 x 5.95	402	391	402
	5.96 x 5.96	400	389	389

The torsional strength of AISI 1020 steel in the cross-sectional dimensions for the cross-sectional angles of 89°, 90° and 91° are shown in Figure 5.

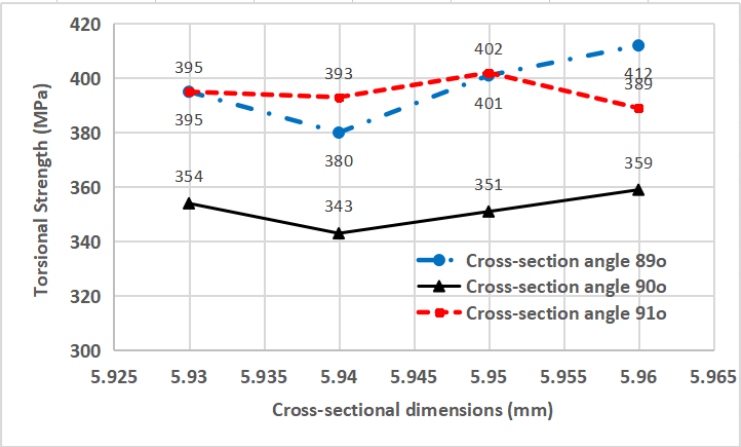

Figure 5. The torsional strength of AISI 1020 steel for the angles of 89°, 90° and 91°

The torsional strength of AISI 1020 steel at an angle of 89° and dimensions of 5.94 mm x 5.94 mm has the lowest torsional strength value at a torsional angle of 720° worth 380 MPa and at dimensions of 5.96 mm x 5.96 mm it has the highest torsional strength at a torsional angle of 720° worth 412 MPa is shown in Table 5 and Figure 6.

Table 5. The torsional strength of AISI 1020 steel at cross-section angles at 89°

No.	Specimen cross-sectional Dimensions (mm)	Twisting Moment			Torsional Strength (MPa)	Maximum Twist Angle (°)
		(kg.m)	(N.m)	(N.mm)		
1	5.93 x 5.93	2.47	24.7	24650	395	680
2	5.94 x 5.94	2.54	25.4	25375	380	720
3	5.95 x 5.95	2.61	26.61	26100	401	720
4	5.96 x 5.96	2.61	26.61	26100	412	720
				Average=	**397**	

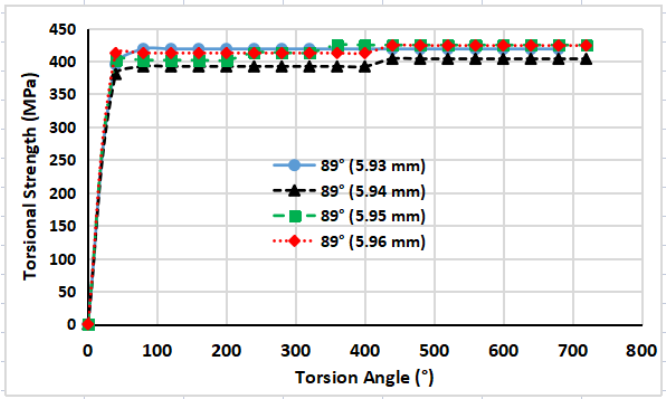

Figure 6. The torsional strength of AISI 1020 steel at a cross-sectional angle of 89°

The torsional strength of AISI 1020 steel at cross-section angles at 90° and dimensions of 5.94 mm x 5.94 mm has the lowest torsional strength value at a torsional angle of 760° worth 343 MPa and at dimensions of 5.96 mm x 5.96 mm it has the highest torsional strength at a torsional angle of 800° worth 359 MPa is shown in Table 6 and Figure 7.

Table 6. Torsional strength of AISI 1020 steel at an angle of cross section at 90°

No.	Specimen cross-sectional Dimensions (mm)	Twisting Moment			Torsional Strength (MPa)	Maximum Twist Angle (°)
		(kg.m)	(N.m)	(N.mm)		
1	5.93	2.47	24.7	24650	354	720
2	5.94	2.39	23.93	23925	343	760
3	5.95	2.47	24.7	24650	351	640
4	5.96	2.54	25.38	25375	359	800
				Average=	**351**	

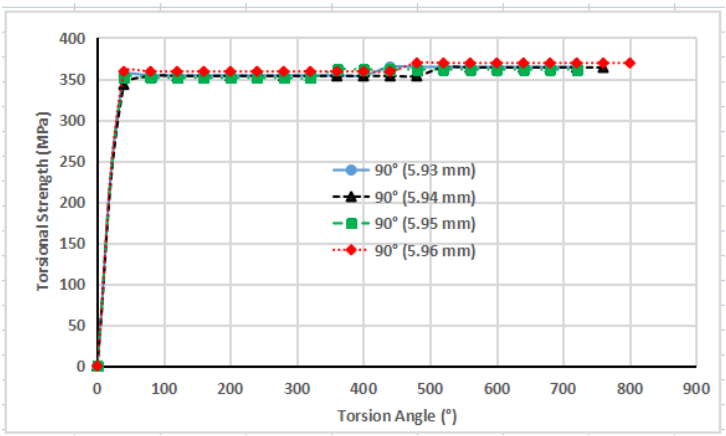

Figure 7. The torsional strength of AISI 1020 steel at a cross-sectional angle at 90°

The torsional strength of AISI 1020 steel at cross-section angles at 91o and dimensions of 5.94 mm x 5.94 mm has the lowest torsional strength value at a torsional angle of 760° worth 393 MPa and at dimensions of 5.95 mm x 5.95 mm it has the highest torsional strength at a torsional angle of 720° worth 402 MPa is shown in Table 7 and Figure 8.

Table 7. Torsional strength of AISI 1020 steel at an angle of cross section at 91°

No.	Specimen cross-sectional Dimensions (mm)	Twisting Moment			Torsional Strength (MPa)	Maximum Twist Angle (°)
		(kg.m)	(N.m)	(N.mm)		
1	5.93	2.47	24.65	24650	395	720
2	5.94	2.47	24.65	24650	393	760
3	5.95	2.54	25.38	25375	402	720
4	5.96	2.47	24.65	24650	389	800
			Average=		**394**	

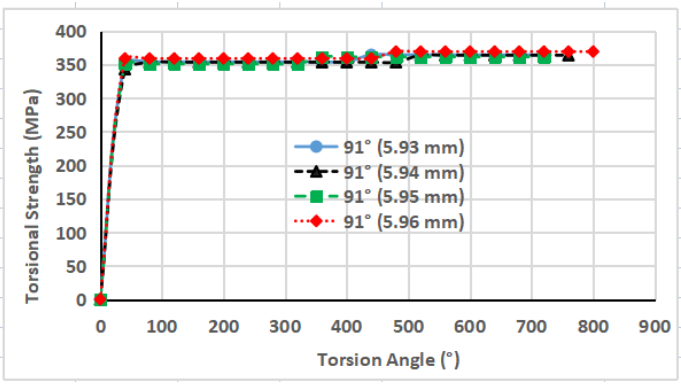

Figure 8. The torsional strength of AISI 1020 steel at cross-sectional angle at 91°

Overall the torsional strength of AISI 1020 steel at cross-section angles at 89° to 91° has a range of values from 343 to 412 MPa or an average of 381 MPa.

The torsional strength of AISI 1020 steel at cross-section angles is not 90° which at cross-section angles 89° increases by 397-351 = 46 MPa or about 13.1% and at cross-section angles 91° it increases by 394-351 = 43 MPa or about 12.3%. So the change in cross-section angles is not 90°, both with a 1° change increase the torsional strength by about 12%.

4. CONCLUSION AND SUGGESTION

The conclusions that can be drawn from the discussion of the torsional strength of AISI 1020 steel at cross-section angles 89°, 9^{0o} and 91° are:
1) Torsional strength is achieved in the range of 351 to 397 MPa;
2) At an angle of 89° the torsional strength increases by 46 MPa or around 13.1 %; and
3) At an angle of 91° the torsional strength increases by 43 MPa or around 12.3 %.

Follow-up suggestions for conclusions include:
1) It is necessary to conduct research on shaft materials other than low carbon steel; and
2) It is necessary to conduct research on the shaft material in the shape of a pipe, either rectangular or cylindrical.

5. REFERENCES

[1] M. B. Widodo, "Analisa perbedaan kekerasan dan ketangguhan baja s45c bila di-quench dan ditemper pada media pendingin udara bertekanan, air dan oli untuk aplikasi poros motor roda tiga," *JTM J. Teknik Mesin Unesa*, vol. 07, no. 03, pp. 105-112, 2021. Available: https://ejournal.unesa.ac.id/index.php/jtm-unesa/article/view/43611.
[2] Ambiyar and Purwanto, *Metal Fabrication*, UNP Press Padang, pp 1-172, 2008.
[3] S. Jatmiko, and S. Jokosisworo, "Analysis of the twisting strength and the twisting flexural strength of the ST 60 steel shaft as a design application for ship propeller shaft materials," *Jurnal Ilmu Pengetahuan dan Teknologi Kelautan*, vol. 5, no. 1, pp. 42-51, 2012. DOI: https://doi.org/10.14710/kpl.v5i1.2666
[4] I. Kurniawan, U. Budiarto, and I. P. Mulyatno, "Analysis of torsional strength, tensile strength, hardness and metallographic tests of S45C steel as material for ship propeller shafts after tempering process," *J. Tek. Perkapalan*, vol. 7, no. 4, pp. 313-322, 2019.

https://ejournal3.undip.ac.id/index.php/naval/article/view/24444
[5] R. R. Putra, S. Jokosisworo, and A. W. Budi, "Analysis of the torsional strength, tensile strength and hardness of ST 60 steel as a material for the propeller shaft after the tempering process," *Tek. Perkapalan*, vol. 6, no. 1, p. 83-90, 2017. Available: http://ejournal3.undip.ac.id/index.php/naval
[6] H. Teimoori, R. T. Faal, and R. Das, "Saint-Venant torsion analysis of bars with rectangular cross-section and effective coating layers," *Appl. Math. Mech.*, vol. 37, no. 2, pp. 237-252, 2016. doi: 10.1007/s10483-016-2028-8. DOI 10.1007/s10483-016-2028-8
[7] T. D. Putra, "Variation of material and size of shaft diameter using torsion testing method," *Widya Tek. Vol.22 No.2;* vol. 22, no. 2, pp. 116-121, 2014. https://publishing-widyagama.ac.id/ejournal-v2/index.php/widyateknika/article/view/117
[8] W. D Callister, *Materials science and engineering an introduction*, Wiley, United States of America, 2014.
[9] K. Macikowski, B. Warda, G. Mitukiewicz, Z. Dimitrova, and D. Batory, "Change in the torsional stiffness of rectangular profiles under bending stress," *Materials (Basel).*, vol. 15, no. 7, pp. 1-18, 2022. doi: 10.3390/ma15072567
[10] R. Bagaskara and M.Fitri, "Modification of the design of metal and composite material torsion testing machines," Jurnal ALMIKANIKA, vol. 5, no. 1, pp. 34-39, 2023. doi: https://doi.org/10.32832/almikanika.v5i1.8924
[11] A. Mustofa, S. Jokosisworo, and A. W. Budi S., "Analysis of tensile strength, flextural strength and torsional strength of ST 41 steel as propeller shaft material after quenching process," *J. Tek. Perkapalan*, vol. 6, no. 1, pp. 199-206, 2018. http://ejournal3.undip.ac.id/index.php/naval
[12] P. Ghavami, *Mechanics of materials: An introduction to engineering technology*. 2015. Available: https://sciarium.com/file/172839/
[13] G. Brabie, "An analysis of the state of stresses generated by torsion in twisted non-circular bars," *J. Mater. Process. Technol.*, vol. 169, no. 3, pp. 401-408, 2005. doi: 10.1016/j.jmatprotec.2005.04.098
[14] Affandi and S. Huzni, "Numerical analysis of low carbon steel torsional strength using software (Solidworks)," *Jurnal Rekayasa Energi Manufaktur*, vol. 6, no. 2, pp. 29-36, 2021. http://doi.org/10.21070/r.e.m.v6i2.1628
[15] F.D. Kristanto-Design of a rotary type material torsional strength test tool, *Skripsi*, Program Studi Mesin Otomotif, Jurusan Teknik, Politeknik Negeri Jember, pp. 1-60, 2020.
[16] V. Kukhar, Y. Sahirov, V. Hornostai, O. Markov, and M. Nahnibeda, "FEM simulation of bending and torsion tests of similar size RHS but of the different production options," *E3S Web of Conferences, ICIES*, vol. 234, no. 00079, 2021. https://doi.org/10.1051/e3sconf/20212340007
[17] Anonymous, "Standars test method for shear modulus at room temperature, Designation: E143-13," Available: https://www.stdlibrary.com/p-142757.html

LOGIC
Journal of Engineering Design and Technology
Vol. 24 No.1 March 2024 ; p. 17 - 23

p-ISSN : 1412-114X
e-ISSN : 2580-5649
http://ojs2.pnb.ac.id/index.php/LOGIC

THE POTENTIALS OF ULTRASONIC ATOMIZER AUGMENTED THE SEA SALT PRODUCTIONS

I Dewa Gede Agus Tri Putra [1)], Putu Wijaya Sunu [2)], Nyoman Sugiartha [1)], Wayan Temaja[1)], I Nyoman Gede Baliarta[1)]

1) Refrigeration And Air Conditioning Study Program, Politeknik Negeri Bali, Jl. Kampus Bukit Jimbaran, Kuta Selatan, Badung, Bali, Indonesia
2) Building Utility Study Program, Politeknik Negeri Bali, Jl. Kampus Bukit Jimbaran, Kuta Selatan, Badung, Bali, Indonesia

Corresponding email [1)]
dewagedeagustriputra@pnb.ac.id

Abstract. Ultrasonic atomizers can potentially augment the production of sea salt through a process known as ultrasonic nebulization. While the traditional method of sea salt production primarily relies on natural evaporation, ultrasonic atomization can accelerate the evaporation process. The process typically involves the following steps: collection of seawater, evaporation, brine crystallization and then harvesting process of the sea salt. After processing, the sea salt is typically dried and packaged for distribution and sale. In this project, the influence of the ultrasonic atomizer in the process of converting saline water into brine, before crystallization, can be assessed. The ultrasonic atomization process significantly increases the surface area of the seawater by converting it into fine droplets. Droplets evaporate more efficient due to large surface area of the droplets. According to testing of the research apparatus which had been conducted, an ultrasonic atomization can increase the salinity by brine evaporation or of droplet productivity of sea salt. This result had been shown in this process can be used to increasing the salinity of sea water. For further steps, this technique can potentially augment the production of sea salt.

Keywords : Ultrasonic, Atomizer, sea salt,evaporation.

1. INTRODUCTION

Sea salt is produced by the evaporation of seawater. The process typically involves the following steps: collection of seawater, filtration, evaporation ponds, evaporation, crystallization and then harvesting process of the sea salt. After processing, the sea salt is typically dried and packaged for distribution and sale [1]. Seawater is collected from the ocean or sea. It is essential to ensure that the water is relatively clean and free from contaminants. The collected seawater is usually passed through a series of filtration systems to remove larger debris, such as sticks, seaweed, and other organic matter. The filtered seawater is then pumped into large, shallow evaporation ponds or basins. These ponds are designed to maximize the surface area of the water exposed to the sun and wind, which accelerates the natural evaporation process. As the seawater sits in the evaporation ponds, it is exposed to sunlight and wind. The sun's heat causes the water to evaporate, leaving behind the dissolved salt and other minerals. The wind helps to concentrate the brine by continually mixing and evaporating the water. As the water evaporates, salt crystals start to form. These crystals are usually a combination of sodium chloride (table salt) and other minerals present in seawater, such as magnesium, calcium, and potassium salts. Once a sufficient amount of water has evaporated, and the salt crystals have formed, they are harvested. This can be done by using rakes, machinery, or even by hand, depending on the scale of production. The harvested salt crystals may contain impurities, such as clay or other minerals. To remove these impurities, the salt is washed and processed. The exact method of processing can vary, but it often involves dissolving the salt in water, filtering it to remove impurities, and then evaporating the water to leave behind pure salt crystals. It's important to note that sea salt can come in various forms, including coarse sea salt, fine sea salt, and specialty sea salts with unique colors and flavors, depending on the specific location and impurities in the seawater. Sea salt is often marketed as a more natural and less processed alternative to table salt, as it retains some of the minerals and elements found in seawater, which can impart distinct flavors and colors to the salt.

Ultrasound has been shown to have a positive effect on the evaporation process of liquids in a vacuum chamber.[2] The use of ultrasound in such processes is often referred to as "sonoevaporation" or "sonochemical evaporation." This technique has several applications in various fields, including chemistry, materials science, and industrial processes. A study conducted by Trushlyakov et al. investigated the process of heat and mass transfer in the evaporation of model liquids (distilled water, alcohol mixture, kerosene TC-1) in a vacuum chamber under parametric ultrasonic influence and vacuum influence on a liquid with the purpose of using the obtained results for the development of methods for designing the evaporation system of unused liquid residues of rocket fuel remaining in the launch vehicle tanks at the end of the mission [3]. The study found that the evaporation rate increases with increasing amplitude of the bath bottom vibrations, with the highest evaporation rate under the same conditions for kerosene TC-1 [3],[4]. Ultrasonic waves create cavitation bubbles in the liquid, which implode and generate shockwaves upon collapse. These shockwaves can increase mass transfer rates, leading to more efficient evaporation. The agitation caused by cavitation bubbles can also prevent the formation of a stagnant layer at the liquid-vapor interface, which can hinder evaporation in a vacuum. Ultrasonic evaporation can be used to promote the crystallization of solutes from a liquid, making it a valuable technique for processes like freeze-drying and also other similar technology. [5],[6].

Ultrasonic Atomizers (UA) can potentially augment the production of sea salt through a process known as ultrasonic nebulization [7], [8]. While the traditional method of sea salt production primarily relies on natural evaporation, ultrasonic atomization can accelerate the evaporation process and improve the yield in controlled environments, such as greenhouses or specialized facilities. In the first step, we can collect and filter seawater to remove larger debris and contaminants, as in traditional sea salt production and then an UA uses high-frequency sound waves to break up liquid into tiny, fine droplets or mist. In sea salt production, seawater will be passed through an ultrasonic nebulizer or atomizer, which creates seawater droplets.[9]

2. METHODS

2.1 Study and Literature Review for Sea Salt Productions Methods

A preliminary study has been conducted to one of the sea salt farming in Kusamba village. This village is a coastal area in the Klungkung regency, Bali province-Indonesia. This village has several farming that produces table salt from sea water in the coastal area of Kusamba bay. Kusamba, a village in the Klungkung region of South Bali, is known for its traditional salt farming practices [10]. The salt farmers in Kusamba use a centuries-old technique to produce 100% natural salt by sun and wind evaporation. The process begins with the farmers repetitively fetching seawater in palm leaf buckets on carrying poles, then splashing them out onto the smoothened black sand under the scorching sun. The salt begins to crystallize after several hours of drying. The mid-day tropical sun bakes the sand into flakes and the salt is ready to be harvested by late afternoon. The farmers take the flakes to the salt-making hut where more seawater is added to leech the salt over several days. The resulting brine is placed in long troughs for further evaporation. The sea salt produced in Kusamba is often characterized by its coarser texture and natural purity. It is typically unrefined and retains some of the minerals and trace elements from the seawater, giving it a unique flavor and appearance. Many people appreciate the taste and quality of this traditional sea salt, which is often sought after for culinary purposes and as a souvenir from the region.

Visitors to Kusamba may have the opportunity to observe the salt farming process and purchase locally produced sea salt as a memento of their visit. It's a traditional and sustainable practice that has been a part of the local culture for generations. Kusamba farmers yield a few kilograms of salts per day on average and the process is dependent to the sunny day, which means it can only be produced during the dry months. Despite the intensive process of sea salt making, Kusamba's salt farmers live in the natural beauty of the beach environmental with shiny-black and mineral-rich sand. This preliminary study also reported that these farmers might be the last generation of salt farmers in Bali since fewer young generations are interested in doing this job. In this study, we are also looking for potentials technology that can increase the capacity of productions of the sea salt farmer. A controllable technology and simply to operate will transform to sustainable salt farming and improving the economic growth of the sea salt farmer.

To increase the salinity of seawater for sea salt production, one of the possible viable strategies is to improve the rate of brine evaporation [11], [12]. The traditional method of harvesting salt relies on the rate of brine evaporation utilizing free solar energy. However, to meet the rising demand for salt, increasing the rate of brine evaporation is one of the possible viable strategies to improve the yield of solar salt production. Several researchers have looked at various methods to enhance the evaporation rate of brine. The various practical approaches reported in the literature for the enhanced brine evaporations are the use of different kinds of materials, mechanical devices, different types of dyes, carbon foam-based porous media, hollow carbon beads, etc. Few literatures discussed the maximum use of renewable energy approaches such as solar energy and wind energy to enhance the brine evaporation [13],[14].

Crystallization is a separation process that relies on the limited solubility of salt in a solvent at a certain temperature and pressure [15]. Nucleation spontaneously commences as the ion concentration exceeds that of the saturated solution. A cluster of crystalline atoms forms firstly in the solution. The crystalline cluster must a attain

mass sufficient free energy to surpass the energy needed to establish an interface between the crystalline phase and the liquid. The nucleation thermodynamics can be understood by considering the interplay between interfacial free energy and the difference in free energy between the liquid and crystal.

2.2 Parameters and Variables for The Phenomenon of Liquid Atomization Ultrasonically

The piezoelectric effect is a phenomenon where certain materials, like quartz or ceramics, generate an electrical charge when subjected to mechanical stress, and conversely, they experience mechanical deformation when an electrical voltage is applied. In ultrasonic atomization, the piezoelectric transducer undergoes various phenomena to create the fine mist. The piezoelectric transducer is driven by an alternating electrical signal, usually at ultrasonic frequencies (higher than 20 kHz). When the electrical voltage is applied to the piezoelectric material, it undergoes rapid mechanical deformation or vibration due to the piezoelectric effect. The transducer's diaphragm or surface oscillates at the same ultrasonic frequency.

Ultrasonic atomization, which involves the generation of fine droplets or mist using high-frequency sound waves, relies on a piezoelectric transducer as an actuator. The piezoelectric effect is a phenomenon where certain materials, like quartz or ceramics, generate an electrical charge when subjected to mechanical stress, and conversely, they experience mechanical deformation when an electrical voltage is applied. In ultrasonic atomization, the piezoelectric transducer undergoes various phenomena to create the fine mist. In the case of ultrasonic atomization of a liquid, the piezoelectric transducer is typically in direct contact with or submerged in the liquid to be atomized. The rapid mechanical vibration of the transducer generates high-frequency pressure waves in the liquid. These pressure waves create tiny, high-velocity liquid jets that break up into fine droplets or mist. This is often referred to as the Rayleigh-Taylor instability, where the liquid jet disintegrates into droplets due to the pressure fluctuations caused by the ultrasonic waves. The size and characteristics of the droplets can be controlled by adjusting the frequency and power of the piezoelectric transducer.

The phenomena of liquids atomization were first reported around 1927. Ultrasonic atomization is a process driven by the intricate interplay of shock waves, vibration amplitude waves, and surface tension, all stemming from the phenomenon of cavitation beneath the liquid's surface. Once the amplitude reaches a critical threshold, tiny droplets are propelled from the wave crest, coalescing into a fine mist. These remarkable ultrasonic atomizers harness the power of ultrasonic waves to transform liquids into minute droplets or a delicate mist, with the ability to fine-tune droplet size simply by selecting the appropriate ultrasonic frequency.[16]

Despite a significant amount of study, the process of droplet formation when exposed to the range ultrasound is still not entirely understood. Two main phenomena have been proposed, such as: cavitation wave and capillary wave. Prior studies proposed the relationship between ultrasonic driven frequency and diameters of droplets. When ultrasonic vibration is reached to a liquid surface, a capillary wave is generated and the wavelength of ultrasounds which is shown by equation [17][18]:

$$\lambda = 0{,}34\left(\frac{8\pi\sigma}{\rho f^2}\right)^{1/3} \quad \text{.....} \quad 1$$

Where λ is the wavelength (m), σ the surface tension (N/m), ρ is the density (kg/m^3) and f is the frequency of surface waves, considered as the half of the device ultrasound frequency. Lang calculated a constant number-of 0.34 for the averaged droplet diameter produced by ultrasound at frequencies between 10 and 800 kHz. The capillary wavelength is consistently divided by the mean diameter.[19]. Then, the constant was modified to 0.96 for averaged droplet diameter of aqueous alcohols solution [20] The average droplet size anticipated by Lang's calculation would fall into multiple micrometer ranges when aqueous solutions were atomized using 1-2 MHz ultrasound.

Another study introduced dimensionless numbers that combined the physico-chemical characteristics of the atomizing liquid with the operating parameters of the ultrasound to propose a connection [21], which is given below:

$$\lambda = \left(\frac{\pi\sigma}{\rho f^2}\right)^{1/3}\left[1 + A(N_{We})^{0.22}(N_{Oh})(N_{In})^{-0.0227}\right] \quad \text{.....} \quad 2$$

N_{we} was defined by weber number and also another dimensionless number (N_{Oh}) was indicated by Ohnesorge number. A Novel dimensional number was defined by Intensity number (N_{In}). it was introduced as an ultrasonic intensity. The Weber number (We) is a dimensionless number in fluid mechanics that is used to analyze fluid flows where there is an interface between two different fluids, especially for multiphase flows with strongly curved surfaces. The Ohnesorge number (Oh) is a dimensionless number that relates the viscous forces to inertial and surface tension forces. it is used to relate to free surface fluid dynamics such as dispersion of liquids in gases and in spray technology.

2.3 Research Apparatus and Devices Measurement

Particularly before the crystallization stage, brine processing is one of important role in sea salt production. It involves concentrating and purifying the brine, which is the highly concentrated saltwater solution, to prepare it for salt crystal formation. Ultrasonic atomization can be employed in various stages of brine processing to enhance efficiency and yield. As the first step, the collected seawater is typically passed through filtration systems to remove larger debris and contaminants. The salinity of this water is typically close to the natural seawater salinity, which is about 35,000 ppm. The seawater is concentrated to increase the salt content (salinity). This concentration is usually done by evaporating some of the water. Ultrasonic atomization can be used to create a fine mist or spray of the concentrated brine. This mist has a higher surface area and facilitates faster evaporation.

The role of ultrasonic atomization in brine processing lies in its ability to create fine sprays or mists that increase the surface area of the liquid exposed to the environment, thus accelerating the evaporation and crystallization processes. This can result in more efficient salt production with potentially higher yields. Ultrasonic atomization also offers the advantage of being controllable and adaptable to different processing conditions. It can help maintain consistent and favorable conditions for salt crystallization and minimize the risk of impurities or uneven crystal formation. Overall, ultrasonic atomization can be a valuable tool in enhancing the brine processing stage of sea salt production, ultimately leading to higher-quality and more efficient sea salt production.

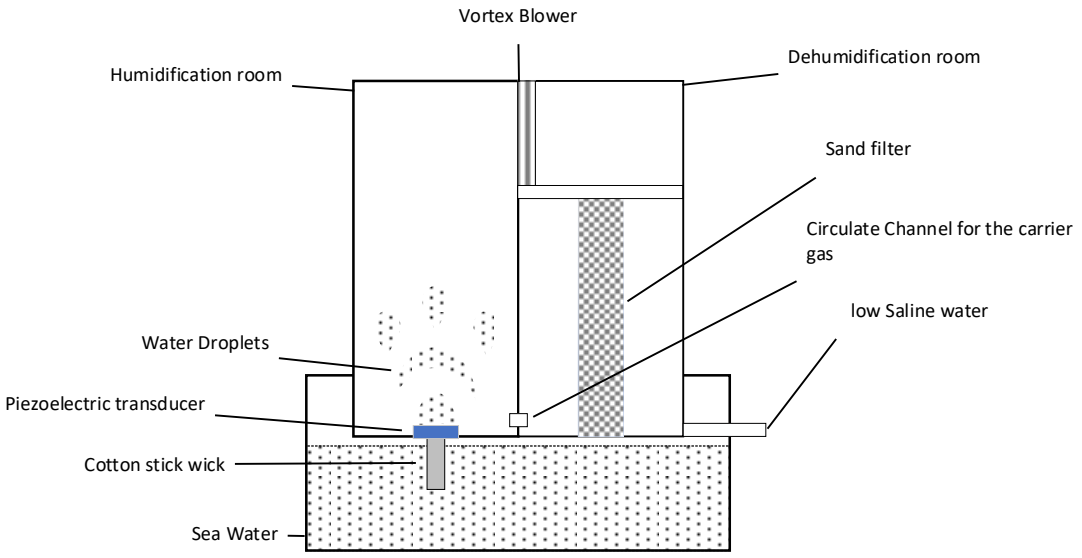

Figure 1. Experimental apparatus for brine production

We have conducted an experimental for understanding the behavior of ultrasonic vibrating mesh in brine processing. This testing apparatus involves two chambers, such as: humidification chamber and dehumidification chamber. The humidification chamber is a chamber that has been installed a piezoelectric. This is an actuator to process atomization ultrasonically. Then in other side, dehumidification chamber will distill the mist into liquid solutions. Measurement devices used in this research to obtain data from brine, include: Total Dissolve Solid (TDS) in water and weighing measurement to indicate the bottom product. TDS of brine solutions were measured by using a portable Digital Salinometer which have wide range measurement 0.00-9.99 ppm and also 1.00 ppt-50.0 ppt. This measurement device depends on the specific research and the type of data being collected. Weighing measurement is a process of determining the output weight of lower saline water, in every 30 minutes data collecting. It also measured the TDS of fresh water production. In the figure 2, schematic of the water purification system has been shown by the functional equipment and the component. An ultrasonic module is needed to drive a piezoelectric transducer ultrasonically.

Distilled water had been used to make initial brine concentrations and number of grams. Normal concentrations of sea water are 35 ppt. We need to prepare brine solutions with a salt concentration of 35 ppt. In this work, we have to add 30 grams sea salt into 1000 ml of distilled water. These solutions will be tested in the apparatus that we have made to carry out the experiment.

3. RESULTS AND DISCUSSION

3.1 Increasing of Salt Concentrations by Ultrasonic Atomization

The process of ultrasonic atomization breaks down the liquid into droplets or mist. These droplets contain a portion of the salt from the original solution, but because they are smaller and spread out, the concentration of dissolved solids in each droplet is lower than in the original liquid [22]. In this testing, the range of Total Dissolved Solids (TDS) of brine water that was prepared has been measured. Brine solutions is 35

ppt. Then, brine water in the container measured for duration time in every 30 minutes. In figure 3, we can show that the number of TDS will be indicated increasing of TDS irregurally in every testing. The average TDS of pure water calculated to 354.6 ppm and the lowest TDS is 35.6 ppm.

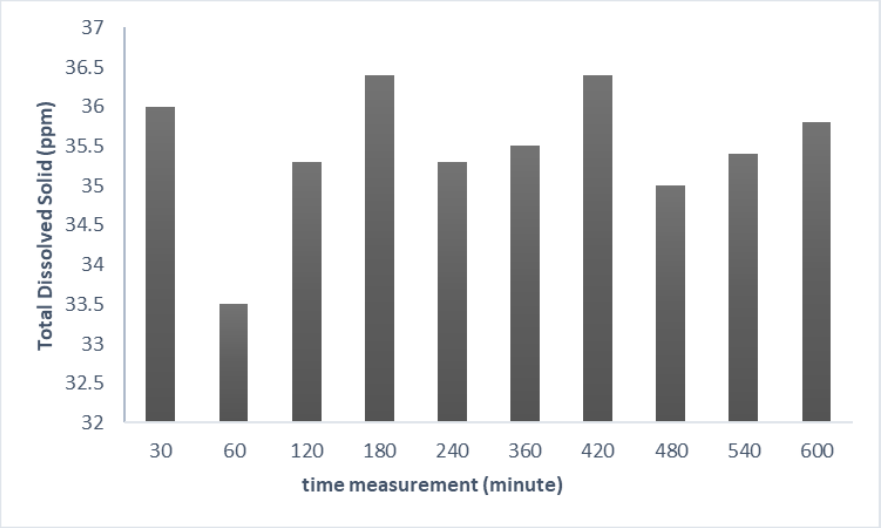

Figure 2. TDS of Brine in container

The specific influence of decreasing TDS will depend on factors such as the initial TDS concentration, liquid properties, atomizer design, and operating conditions. Therefore, it is recommended to conduct thorough experimental investigations or consult scientific literature for a more detailed understanding of the influence of decreasing TDS in a specific application. The presence of dissolved solids in a liquid can affect the size distribution and uniformity of the atomized droplets. Higher TDS levels may result in larger droplets or uneven spray patterns. By reducing TDS, it is possible to achieve finer droplet sizes and more consistent spray characteristics.

3.2. Productions Rate of Brine

This experiment was carried out by utilizations of apparatus that due to brine solutions as the bottom's product. Measurement of brine concentrations will be indicated by the reductions of TDS in saline water output. Flow rate of saline water will be reaching the minimization of brine. Even though, it can be analyzed to the brine productions as other part of productions output.

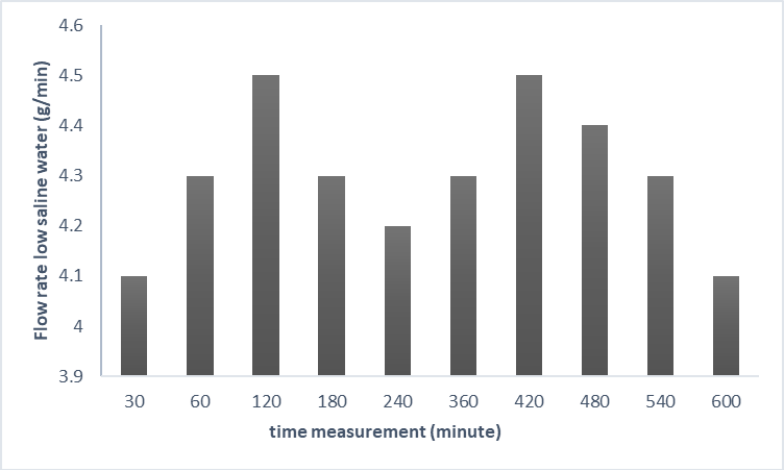

Figure 3. Flow Rate of saline water output

Figure 3 show that the irregular conditions conclude in the collecting of the low salinity water output. The design of this apparatus led to difficulty of collecting the output of low salinity water. Residue of the pure water has been inhibited when collect the output. The average output flow rate is 4.3 g/min. After 10 hours of

testing, 1 liter of saline water can be separated to 0.8 l of brine solutions (36.5 ppm). This technique can produce brine as bottom product with 80% efficiency rate.

Ultrasonic vibrating mesh can improve liquid separation techniques through a phenomenon known as ultrasonic atomization. When a liquid layer or dense liquid is subjected to power ultrasound, fine mist is produced from the liquid surface. This process is characterized by the following points:

- Very fine droplets, ranging from several to several tens of micrometers in size, are obtained with a narrower size distribution.
- There is no need to pressurize the fluid, making the equipment simpler.
- The droplet density and transfer can be easily controlled.
- Ultrasonic atomization is used in various fields that require fine droplets or aerosols due to their small size and narrow size distribution. Compared to conventional nozzles that use high shear to break up liquid, ultrasonic at-omization produces smaller droplets with a narrower size distribution [19],[20]. The phenomenon of atomization by vibrating meshing occurs in frequency 120 kHz as the frequency that generates by ultrasonic module. It enables solute partitioning between mist and bulk liquid, which has led to new aspects of separation in ultrasonic atomization.

3.3. Disadvantages to Transfers this Technology into the Industrial Practice

Brine preparation ultrasonically is a relatively recent technique. More research and analysis will be required by researchers to make ultrasonic systems easier to design. They must continue to build theoretical data models in order to standardize the design of ultrasonic devices. Once these models are created, we will be able to use ultrasonic devices more regularly. Most significantly, we will be able to scale them up to filter larger amounts of water.

Ultrasonic technology can be expensive to maintain. This is related to the repair and maintenance of the ultrasound probe, which becomes damaged during ultrasonic activity. If ultrasonic devices fail, they may require the services of an expert to be repaired. This requirement may cause a region to be without water treatment for an extended period of time. As a result, technologies that are less expensive and easier to fix are becoming increasingly popular. Hopefully, ultrasonic technology will become more widely available, dependable, and economical. This technique is yet another useful instrument for making sea salt for household appliances.

4. CONCLUSION

The potentials of ultrasonic atomization in brine processing lies in its ability to create fine sprays or mists that increase the surface area of the liquid exposed to the environment, thus accelerating the evaporation and crystallization processes. This can result in more efficient salt production with potentially higher yields. Ultrasonic atomization also offers the advantage of being controllable and adaptable to different processing conditions. It can help maintain consistent and favorable conditions for salt crystallization and minimize the risk of impurities or uneven crystal formation. Overall, ultrasonic atomization can be a valuable tool in enhancing the brine processing stage of sea salt production, ultimately leading to higher-quality and more efficient sea salt production.

5. ACKNOWLEDGEMENT

Author would like to thanks for financial support by The Ministry of Education, Culture, Research and Technology under the grant no: 162/SPK/D.D4/PPK.01.APTV/VI/2023.

6. REFERENCES

[1] I. Muhandhis, B. Wirjodirdjo, E. Suryani, H. Susanto, and U. Asfari, “Modeling of Salt Supply Chains to Achieve Competitive Salt Prices,” *Int. J. Food Syst. Dyn.*, vol. 12, no. 1, pp. 51–67, 2021, doi: 10.18461/ijfsd.v12i1.75.

[2] C. Binnie, M. Kimber, and H. Thomas, “Activated carbon adsorption,” in *Basic Water Treatment*, ICE Publishing, 2017, pp. 147–155.

[3] V. I. Trushlyakov, I. Y. Lesnyak, A. A. Novikov, and C. Spada, “Investigation of the liquid evaporation process in a vacuum chamber with ultrasound influence,” *J. Phys. Conf. Ser.*, vol. 1210, no. 1, 2019, doi: 10.1088/1742-6596/1210/1/012146.

[4] S. G. Babu, M. Ashokkumar, and B. Neppolian, “The role of ultrasound on advanced oxidation processes,” *Top. Curr. Chem.*, vol. 374, no. 5, pp. 1–32, 2016, doi: 10.1007/s41061-016-0072-9.

[5] S. Scharnowski and C. J. Kähler, "Particle image velocimetry - Classical operating rules from today's perspective," *Opt. Lasers Eng.*, vol. 135, no. November 2019, p. 106185, 2020, doi: 10.1016/j.optlaseng.2020.106185.
[6] M. D. Protheroe and A. M. Al-Jumaily, "Ultrasound effect on droplet evaporation," *ASME Int. Mech. Eng. Congr. Expo. Proc.*, vol. 3–2015, pp. 2015–2018, 2015, doi: 10.1115/IMECE2015-50552.
[7] I. D. G. A. T. Putra, P. W. Sunu, I. W. Temaja, N. Sugiartha, I. M. Sugina, and I. W. Suirya, "Investigation on application of ultrasonic humidifier for air conditioning system," *J. Phys. Conf. Ser.*, vol. 1450, no. 1, 2020, doi: 10.1088/1742-6596/1450/1/012050.
[8] J. Zhang, Q. Yan, and W. Sun, "Advances in Piezoelectric Atomizers," *Trans. Nanjing Univ. Aeronaut. Astronaut.*, vol. 37, no. 1, pp. 54–69, 2020, doi: 10.16356/j.1005-1120.2020.01.005.
[9] S. Hsieh, C. Huang, and Y. Lu, "Water spray heat transfer through a piezoelectric atomizer with a single-hole micronozzle," vol. 34, no. 8, 2020, doi: 10.1007/s12206-020-0735-x.
[10] T. Akinaga, S. C. Generalis, C. Paton, O. N. Igobo, and P. A. Davies, "Brine utilisation for cooling and salt production in wind-driven seawater greenhouses: Design and modelling," *Desalination*, vol. 426, no. October 2017, pp. 135–154, 2018, doi: 10.1016/j.desal.2017.10.025.
[11] B. G. Vyas, P. K. Labhasetwar, A. Yadav, and A. R. Paital, "A compendium of evaporation techniques for salt production from seawater and sub-soil brine," *Chem. Pap.*, vol. 76, no. 11, pp. 6659–6674, 2022, doi: 10.1007/s11696-022-02363-1.
[12] N. A. Pambudi, J. Yusafiadi, M. K. Biddinika, Y. Estriyanto, and A. Sarifudin, "An experimental investigation of salt production improvement by spraying and heating," *Case Stud. Therm. Eng.*, vol. 30, no. December 2021, p. 101739, 2022, doi: 10.1016/j.csite.2021.101739.
[13] X. Ma, L. Wang, Z. Zhao, S. Liang, and H. Zheng, "A small heat capacity solar distiller with extra effective discharge for brine by the siphoning of a hydrophilic membranous wick," *Desalination*, vol. 521, no. April, p. 115306, 2022, doi: 10.1016/j.desal.2021.115306.
[14] J. Xu *et al.*, "Solar-driven interfacial desalination for simultaneous freshwater and salt generation," *Desalination*, vol. 484, no. December 2019, p. 114423, 2020, doi: 10.1016/j.desal.2020.114423.
[15] G. Liu *et al.*, "Salt-Rejecting Solar Interfacial Evaporation," *Cell Reports Phys. Sci.*, vol. 2, no. 1, p. 100310, 2021, doi: 10.1016/j.xcrp.2020.100310.
[16] M. Ashokkumar *et al.*, "Handbook of ultrasonics and sonochemistry," *Handb. Ultrason. Sonochemistry*, pp. 1–1487, 2016, doi: 10.1007/978-981-287-278-4.
[17] H. Naidu, O. Kahraman, and H. Feng, "Novel applications of ultrasonic atomization in the manufacturing of fine chemicals, pharmaceuticals, and medical devices," *Ultrason. Sonochem.*, vol. 86, no. January, p. 105984, 2022, doi: 10.1016/j.ultsonch.2022.105984.
[18] Y. Da Lang and J. H. Zhang, "Influence of piezoelectric atomizer pores on ultrasonic atomization effect," *Proc. 2014 Symp. Piezoelectricity, Acoust. Waves Device Appl. SPAWDA 2014*, pp. 287–290, 2014, doi: 10.1109/SPAWDA.2014.6998582.
[19] J. Lano, "Ultrasonic Atomization of Liquids An experimental study was made of the mechanism by which the ultrasonic vibration of liquid surfaces on the liquid surface when atomization diameter of the particles produced was found to be a constant fraction , of the c," *Acustica*, vol. 341, no. 1954, pp. 28–30, 1962.
[20] K. Yasuda, K. Mochida, Y. Asakura, and S. Koda, "Separation characteristics of alcohol from aqueous solution by ultrasonic atomization," *Ultrason. Sonochem.*, vol. 21, no. 6, pp. 2026–2031, 2014, doi: 10.1016/j.ultsonch.2014.02.011.
[21] R. Rajan and A. B. Pandit, "Correlations to predict droplet size in ultrasonic atomisation," *Ultrasonics*, vol. 39, no. 4, pp. 235–255, 2001, doi: 10.1016/S0041-624X(01)00054-3.
[22] M. Efstratiou, J. Christy, and K. Sefiane, "Crystallization-Driven Flows within Evaporating Aqueous Saline Droplets," *Langmuir*, vol. 36, no. 18, pp. 4995–5002, 2020, doi: 10.1021/acs.langmuir.0c00576.

LOGIC
Journal of Engineering Design and Technology
Vol. 24 No.1 March 2024 ; p. 24 - 30

p-ISSN : 1412-114X
e-ISSN : 2580-5649
http://ojs2.pnb.ac.id/index.php/LOGIC

ASSESSING MUSCULOSKELETAL DISORDERS (MSDS) OF WORKERS OF FIRED CLAY BRICKS INDUSTRY

Tri Budiyanto[1)], Okka Adiyanto[1)], Farid Ma'ruf[1)], Hari Haryadi[2)], Dimas Yudhafinanto Putra[1)]

1) Industrial Engineering Department, Universitas Amad Dahlan, Yogyakarta, Indonesia
2) Food Technology Department, Universitas Amad Dahlan, Yogyakarta, Indonesia

Correponding email [1)] : Okka.adiyanto@ie,.uad.ac.id

Abstract. Ergonomics is important for sustainable development in many fields, including architecture, health, product design, safety, and workplace design. Ergonomic assessments are essential in the workplace to prevent musculoskeletal disorders (MSDs). Currently, Indonesia has a standardized ergonomic assessment, SNI 9011:2021. This assessment standard is widely used to evaluate human posture. This study aims to evaluate the position of a traditional brick-maker in which the posture identification system is based on the SNI 9011:2021. This study employed a cross-sectional design with a sample of workers in conventional brick manufacturing. The primary findings of this study were visual ergonomic assessment for posture identification, identification of ergonomic assessment categories with high risk in brick manufacturing, and the prevalence of nagging pain among workers in the brick moulding and drying process. To reduce occupational ergonomic risk, particularly for brick-making workers, ergonomic intervention is required in the form of additional work aids such as chairs. This has been shown to reduce the evaluation score based on SNI 9011: 2021, thereby reducing the occurrence of musculoskeletal disorders.

Keywords : Ergonomic, Musculoskeletal disorder, SNI 9011:2021, brick industry,

1. INTRODUCTION

Ergonomics is important in many fields, including product design, architecture, health and safety, and workplace design [1,2]. Ergonomic assessment is a significant component in preventing musculoskeletal disorders (MSDs). Musculoskeletal disorders (MSDs) have been a major health concern that is frequently caused or exacerbated by workplace factors such as repetitive motion, stress, and awkward postures [3-5]. These disorders are associated with decreased productivity, sick leave, and chronic work disability [6,7]. MSDs can lead to pain and impaired function in the musculoskeletal system, particularly in the upper extremities and neck [8,9]. Recognizing the underlying causes and risk factors of MSDs is imperative for effective treatment and prevention. An ergonomic assessment is widely used to examine the human joint skeleton and identify postures that help prevent MSDs. Many ergonomic assessments are currently taking place in a variety of sectors. One of the industries that receives a lot of complaints about MSDs is industrial manufacturing.

Personal factors and ergonomics have long been important considerations in the industrial sector. In the manufacturing industry, it will affect the working productivity in which the manufacturing sector will rely heavily on output, product quality, and innovation [10]. This manufacturing sector requires efficient use of human resources to achieve high productivity [11].

Musculoskeletal disorders (MSDs) represent a significant health problem, often caused or exacerbated by work-related factors such as repetitive movements, stresses, and clumsy postures [12,13]. These impairments can

lead to decreased productivity, sickness absence, and chronic work disability [12]. Dental professionals are particularly vulnerable to MSDs due to the suboptimal ergonomics of the work environment [14]. The impact of MSDs on the musculoskeletal system can be resulting in pain and impaired function, especially in the upper extremities and neck [13]. Thus, understanding the causes and risk factors of MSDs is essential for effective intervention and prevention.

Human resources are a critical component of a manufacturing industry's production activities. To increase productivity and quality, consider the environment, workspace, and operator conditions. This will have a significant impact on the operator's physical conditions they also require adequate rest time to work, which increases labour productivity [10,15].

Various work environment factors are likely to contribute to the development of MSDs in the brick making process. Certain body sites such as the neck, upper extremities, and back have a high increased risk of MSDs [16] These impairments are associated with risk factors in the work environment including lifting, material handling, repetitive work postures, and awkward work postures. Excessive repetitive and prolonged exposure to static loads can lead to complaints of damage to joints, ligaments and tendons. Workers who perform repetitive activities in one cycle are very vulnerable to MSDs [17].

Brick-making is one example of a physically demanding activity. Workers in the brick-making of small and medium enterprise (UMKM) continue to engage in manual activity. This industry continues to be supported by a large number of workers as well as the use of traditional equipment in the burning and drying processes. The brick production process continues to use traditional tools, such as a manual printing process that is done in a sitting position for 7 hours. This can lead to the occurrence of MSDs.

The working system that has been in place for generations to maintain this commitment presents a challenge in improving work postures that can lead to MSDs. Some of them perform in the brick industry. Work posture in a sitting position during the brick-making process is one of the risks of MSDs. Consequently, the company owner's intervention is required in order to consider humans as the primary driver of improvement while maintaining the value of the work culture that workers have long maintained.

Several studies on MSDs have been carried out. A large percentage of workers who have worked for 4.5 years or have reached the age of 30 experience health and physical deterioration as as a consequence of their workload. However, once workers become accustomed to their working conditions, they no longer perceive these complaints [18]. Workers' main complaints after work concern the waist, neck, and certain parts of the spine [19,20].

Risk assessment is an advantageous instrument for investigating unfavorable workplace exposures and prioritizing workplace changes. Health and safety legislation in Sweden and Europe requires periodic risk assessments to prevent exposure to potentially hazardous work environments [21,22]. SNI 9011: 2021 is one of the risk assessments that has become a standard in Indonesia. It is a standard for identifying ergonomic hazards. SNI 9011: 2021 measures the stages of preparation, implementation, and evaluation of ergonomic measurements in the workplace. The findings of this study can be used to identify potential health issues caused by ergonomic hazards in the workplace [23]. Thus, the purpose of this study is to identify MSD disorders in brick-making workers using SNI 9011: 2021, which was issued by the Indonesian government.

2. METHODS

This research design was cross-sectional involving 47 participants from the Yogyakarta geographic region. Respondent participation was based on consent and a protocol approved by Ahmad Dahlan University's ethics committee on October 25, 2023 (number 012310241). The selection of respondents was carried out randomly from the existing population. Assessment of MSDs and ergonomic symptoms refers to SNI 9011-2021, which addresses the assessment and evaluation of ergonomic risks in the workplace. Appendix D: SNI 9011-2021 contains an ergonomic hazard questionnaire for analysing and evaluating the level of ergonomic risk. The study looked at exposure duration, manual handling, and upper and lower body posture. Table 1 displays the total score based on the ergonomic risk level evaluation results.

Table 1. Risk Level Interpretation.

Score	Interpretation
≤ 2	Safe workplace
3-6	Need further Assessment
≥ 7	Dangerous

3. RESULTS AND DISCUSSION

3.1 Characteristic Respondent

The characteristics of research respondents are required to determine the distribution of respondents. Age measurements on the KTP are based on the date of birth, while gender is a phenotypic trait indicated by secondary gender characteristics. Body weight and height measurements were taken during the study. The research included 47 participants with an average age of 55±5.18 years. In this study's age variable, there were 40 people over 50 (85.1%) and 7 people under 50 (14.9). Male workers totalled 29 (61.7%), while female workers totalled 18 (38.3%). Further details, the characteristics of the respondents are shown in Table 2.

Table 2. The Characteristic of Respondent

Parameters	Mean ± SD
Age (Years)	55 ± 5.18
Height (cm)	153.47 ± 7.61
Weight (Kg)	57.27 ± 8.95
BMI (Kg/m2)	24.37 ± 3.48
Work Experience (Years)	12.40 ± 4.67

3.2. Gender

In the study, 47 people took part in brick making. In this study, 61.7% were men and 38.3% were women. According to the study's findings, female respondents reported experiencing more MSD symptoms in the previous year while working on brick making. Some studies have also found that women are more likely to develop MSD symptoms when engaging in repetitive activities [24,25].

3.2. Working Periods

The working period in the brick industry is a considerable length of time, it can be seen in Table 2 that the average working period of the workers is 12.4 years. According to research [17], there is a relationship between length of service and MSDs, especially work involving muscle strength.

3.3. Ergonomic Risk Assessment

The assessment of potential ergonomic risks in brick-making based on SNI 9011-2021 identifies two assessment categories that are high risk and warrant further investigation. According to the results of the musculoskeletal disorders analysis, the hazard level score ranged from 7 to 26, with a total of 47 respondents. In the assessment of MSD symptoms in the process of printing and drying bricks, it was discovered that 6.4% of the sample never felt annoying pain caused by the work of printing and drying bricks, while the remaining 93.6% experienced undesirable pain as a side effect of the work of printing and drying bricks. Of the total respondents, 44 workers experienced pain (93.6%) and the remaining 3 workers did not suffer from pain (6.4%). The number of hours spent at work by the respondents was 32 people doing their work for more than 5 hours (68.1%), while the remaining 15 people worked for less than 5 hours (31.9). Most of the respondents, namely 42 people, use their right hand as the dominant hand (89.4%) while the remaining 3 respondents use their left hand as the dominant hand (6.4%) and there are also right and left hand dominant workers, as many as 2 respondents (4.2%). A total of 44 respondents have worked for more than 5 years (93.6%) and 3 respondents have worked for less than 5 years (6.4%).

Figure 1. Work posture of brick worker

Workers in the brick sector experience MSDs complaints as a result of repetitive activities during the brick moulding process, which put pressure on the muscles due to the continuous workload. Furthermore, it is the result of working postures while sitting during the moulding process. Symptoms of MSDs based on SNI 9011-2021 revealed that as many as 6.4% of the sample never experienced annoying pain caused by the work of printing and drying bricks, while the remaining 93.6% experienced annoying pain as a result of the work. Of the 6% of the workers who did not experience pain, two had not worked for more than ten years, and one had worked for more than ten years but could use both hands well without dominant left or right hands making the worker's job easier. Figure 2 illustrates the results of pain complaints.

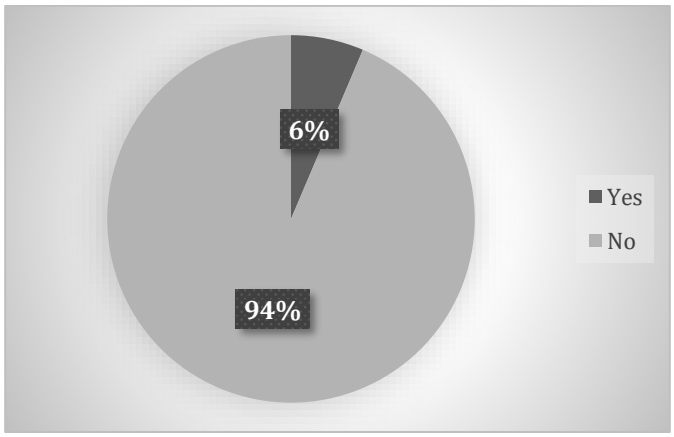

Figure 2. The chart of pain complaint

Static postures put more strain on muscles and tendons, resulting in fatigue or exhaustion [26,27]. The hazard score in the gotrak assessment work posture ranges from a maximum of 26 to a minimum of 7, with a tolerance value of less than 7 indicating safety.

Figure 3. Photo of workers after using suggested improvements

Figure 4. Picture of worker mannequin after suggested improvements

The suggested improvement to the type of folding chair has a significant impact on the hazard factor score assessment. Whenever this improvement suggestion is implemented, all overall ratings for the hazard factors will change. For instance, the respondent's hazard factor score began with a value of 8, which is classified as hazardous, but after implementing the improvement suggestion in the form of a folding chair, the score changed from 8 to 6. Based on the results of the SNI 9011-2021 assessment, it is demonstrated that the improvement suggestion in the form of a folding chair can reduce the hazard factor score.

4. CONCLUSION

The results of the MSD assessment using SNI 9011-2021 show that most traditional brick-makers have MSDs symptoms with varying degrees of risk. As many as 93.6% of workers complain of lower back pain, which is caused by their position, specifically crouching. The average age of brick workers is more than 50 years. The advice assigned to reduce MSDs complaints is to provide a small chair to sit in while making bricks. The score obtained before using a small chair was 8, and the score obtained after using a chair as a seat was 6. This illustrates how suggestions for improvement, such as using a chair or sitting aid, can reduce the score value of MSDs complaints based on SNI 9011 2021.

Therefore, it is recommended that brick-making workers require ergonomic intervention in the form of additional work aids such as chairs to reduce work ergonomic risks. This has been proven to reduce evaluation scores based on SNI 9011:2021 thereby reducing the occurrence of musculoskeletal disorders.

5. ACKNOWLEDGEMENT

The authors are grateful to Universitas Ahmad Dahlan for funding the research with the nomor PD-232/SP3/LPPM-UAD/VIII/2023.

6. REFERENCES

[1] Rathore, B., Pundir, A. K., & Iqbal, R. (2020). Ergonomic risk factors in glass artware industries and prevalence of musculoskeletal disorder. *International Journal of Industrial Ergonomics*, 80(September), 103043. https://doi.org/10.1016/j.ergon.2020.103043

[2] Taifa, I. W., & Desai, D. A. (2017). Anthropometric measurements for ergonomic design of students' furniture in India. *Engineering Science and Technology, an International Journal*, 20(1), 232–239. https://doi.org/10.1016/j.jestch.2016.08.004

[3] Kusumawardhani, A., Djamalus, H., & Lestari, K. dani. (2023). Ergonomic Risk Assessment and MSDs Symptoms Among Laboratory Workers Using SNI 9011-2021. *Indonesian Journal of Occupational Safety and Health*, 12(May), 35–41. https://doi.org/10.20473/ijosh.v12iSI1.2023.35-41

[4] Qureshi, A., Manivannan, K., Khanzode, V., & Kulkarni, S. (2019). Musculoskeletal disorders and ergonomic risk factors in foundry workers. *International Journal of Human Factors and Ergonomics*, 6(1), 1–17. https://doi.org/10.1504/IJHFE.2019.099579

[5] Rajendran, M., Sajeev, A., Shanmugavel, R., & Rajpradeesh, T. (2021). Ergonomic evaluation of workers during manual material handling. *Materials Today: Proceedings*, 46, 7770–7776. https://doi.org/10.1016/j.matpr.2021.02.283

[6] Daneshmandi, H., Choobineh, A. R., Ghaem, H., Alhamd, M., & Fakherpour, A. (2017). The effect of musculoskeletal problems on fatigue and productivity of office personnel: A cross-sectional study. *Journal of Preventive Medicine and Hygiene*, 58(3), E252–E258. https://doi.org/10.15167/2421-4248/jpmh2017.58.3.785

[7] Das, B. (2021). Improved work organization to increase the productivity in manual brick manufacturing unit of West Bengal, India. *International Journal of Industrial Ergonomics*, 81(March 2020), 103040. https://doi.org/10.1016/j.ergon.2020.103040

[8] Dale, A. M., Strickland, J., Gardener, B., Symazik, J., & Evanoff, B. (2010). Exposures of the Upper Extremity. *International Journal Occuptaional Environmental Health*, 16(August 2007), 1–10.

[9] Karukunchit, U., Puntumetakul, R., Swangnetr, M., & Boucaut, R. (2015). Prevalence and risk factor analysis of lower extremity abnormal alignment characteristics among rice farmers. *Patient Preference and Adherence*, 9, 785–795. https://doi.org/10.2147/PPA.S81898

[10] Boulila, A., Ayadi, M., & Mrabet, K. (2018a). Ergonomics study and analysis of workstations in Tunisian mechanical manufacturing. *Human Factors and Ergonomics In Manufacturing*, 28(4), 166–185. https://doi.org/10.1002/hfm.20732

[11] Salimi, F., Sheikhmozafari, M. J., Tayebisani, S., & Ahmadi, O. (2021). Risk Assessment of Musculoskeletal Disorders Prevalence in Female Hairdressers using RULA and NERPA Techniques. *International Journal of Musculoskeletal Pain Prevention*, 6(3), 545–553. https://doi.org/10.52547/ijmpp.6.3.545

[12] Kim, S., Lee, H., Hong, K., & Lee, Y. (2015). Use of three-dimensional technology to construct ergonomic patterns for a well-fitting life jacket of heterogeneous thickness. *Textile Research Journal*, *85*(8), 816-827.

[13] Korhan, O., & Memon, A. A. (2019). Introductory chapter: work-related musculoskeletal disorders. In *Work-related musculoskeletal disorders*. IntechOpen.

[14] Leslie, S., de Castro Abreu, A. L., Chopra, S., Ramos, P., Park, D., Berger, A. K., ... & Aron, M. (2014). Transvesical robotic simple prostatectomy: initial clinical experience. *European urology*, *66*(2), 321-329.

[15] Boulila, A., Ayadi, M., & Mrabet, K. (2018b). Ergonomics study and analysis of workstations in Tunisian mechanical manufacturing. *Human Factors and Ergonomics In Manufacturing*, 28(4), 166–185. https://doi.org/10.1002/hfm.20732

[16] Trianni, A., Cagno, E., Neri, A., & Howard, M. (2019). Measuring industrial sustainability performance: Empirical evidence from Italian and German manufacturing small and medium enterprises. *Journal of Cleaner Production*, 229, 1355–1376. https://doi.org/10.1016/j.jclepro.2019.05.076

[17] Oliv, S., Gustafsson, E., Baloch, A. N., Hagberg, M., & Sandén, H. (2019). The Quick Exposure Check (QEC) — Inter-rater reliability in total score and individual items. *Applied Ergonomics*, 76(December 2018), 32–37. https://doi.org/10.1016/j.apergo.2018.11.005

[18] Moriguchi, C. S., Sato, T. O., Coury, H. J. C. G., Taifa, I. W., Desai, D. A., Deros, B. M., Daruis, D. D. I., Basir, I. M., Enez, K., Nalbantoğlu, (2019). Impact of experience when using the Rapid Upper Limb Assessment to assess postural risk in children using information and communication technologies. *International Journal of Industrial Ergonomics*, 70(December 2018), 398–405. https://doi.org/10.1016/j.apergo.2013.05.004

[19] Chen, J. D., Falkmer, T., Parsons, R., Buzzard, J., & Ciccarelli, M. (2014). Impact of experience when using the Rapid Upper Limb Assessment to assess postural risk in children using information and communication technologies. *Applied Ergonomics*, 45(3), 398–405. https://doi.org/10.1016/j.apergo.2013.05.004

[20] Adiyanto, O., Mohamad, E., Jaafar, R., & Faishal, M. (2023). Identification of Musculoskeletal Disorder among Eco-Brick Workers in Indonesia. *International Journal of Occupational Safety and Health*, 0878, 29–40.

[21] Kristanto, A., Bariyah, C., & Kurniawan, A. (2023). Biomechanical evaluation of rice farmers during paddy threshing activity. *Journal of Current Science and Technology*, 13(1), 12–22.

[22] Coenen, P., Gilson, N., Healy, G. N., Dunstan, D. W., & Straker, L. M. (2017). A qualitative review of existing national and international occupational safety and health policies relating to occupational sedentary behaviour. *Applied ergonomics*, *60*, 320-333.

[23] Ramaganesh, M., Jayasuriyan, R., Rajpradeesh, T., Bathrinath, S., & Manikandan, R. (2021). Ergonomics hazard analysis techniques-A technical review. *Materials Today: Proceedings*, *46*, 7789-7797.

[24] Susanto, A., Komara, Y. I., Mauliku, N. E., Khaliwa, A. M., Asep, D., Syuhada, A. D., & Putro, E. K. (2022). Measurement and Evaluation of Potential Ergonomic Hazards in The Analytical & Assay Laboratory of The Concentrating Division. *Journal of Industrial Hygiene and Occupational Health*, 7(1), 36–52.

[25] Davison, C., Cotrim, T. P., & Gonçalves, S. (2021). Ergonomic assessment of musculoskeletal risk among a sample of Portuguese emergency medical technicians. *International Journal of Industrial Ergonomics*, 82(November 2020), 103077. https://doi.org/10.1016/j.ergon.2020.103077

[26] Asshidiq, E., & Nur Rahman As'ad. (2023). Identifikasi Risiko Kerja dan Keluhan Gangguan Otot Rangka Pekerja Kios Berkah Jaya. *Bandung Conference Series: Industrial Engineering Science*, 3(1), 348–355. https://doi.org/10.29313/bcsies.v3i1.6789

[27] Marras, W. S., Lavender, S. A., Ferguson, S. A., Splittstoesser, R. E., & Yang, G. (2010). Quantitative dynamic measures of physical exposure predict low back functional impairment. *Spine*, 35(8), 914–923. https://doi.org/10.1097/BRS.0b013e3181ce1201

LOGIC
Journal of Engineering Design and Technology
Vol. 24 No.1 March 2024 ; p. 31 - 38

p-ISSN : 1412-114X
e-ISSN : 2580-5649
http://ojs2.pnb.ac.id/index.php/LOGIC

ENHANCING ESSENTIAL OIL YIELD: UTILIZING INTERNAL CHOPPER IN STEAM DISTILLATION

IM Rajendra [1)], IA Anom Arsani [1)], IM Sudana [1)], IGN Suta Waisnawa [1)]

[1)] Mechanical Engineering Department, Politeknik Negeri Bali, Kuta Selatan, Bali, Indonesia 80646

Coressponding Author:
maderajendra@pnb.ac.id

Abstract. Distillation will be optimal if the raw material has a large surface area, for this it requires a chopping process. The aim of this research is to investigate the increase in oil yield achieved through steam distillation with the integration of a chopping module which is a novel distillation process. To achieve this, we employed a distillation reactor equipped with an internal chopping module to enhance both the quantity and quality of Champaca essential oil production. Our experiments involved three variations of pre-distillation treatment: no chopping, chopping inside the reactor, and chopping outside the reactor. The distilled oil was subsequently analyzed using GC-MS. These three chopping methods resulted in varying amounts of Linalool compounds. Unchopped essential materials yielded 6.54% Linalool compounds, while internal chopping produced 32.33%, and external chopping resulted in 7.40% Linalool compounds. The internal chopping method proved to be the most effective in increasing Linalool compound content. Consequently, we can conclude that chopping materials within the distillation reactor during the steam distillation process can increase the main compound's content.

Keywords : Essential Oil, Steam Distillation, Champaca Oil, Chopper

1. INTRODUCTION

As an agricultural country, Indonesia possesses abundant natural plant resources. Among these resources are plants that produce essential oils. There are nearly 150 plants known for their essential oil production, with 40 of them being actively cultivated and exported [1]. Essential oils, also referred to as volatile oils, are extracted from various parts of plants, including leaves, flowers, wood, seeds, or flower buds, through a distillation process. Essential oil extraction methods include steam distillation, distillation, or extraction, which separate the aromatic compounds from the raw materials. The resulting product is an oil containing highly concentrated active compounds, such as aromatic terpenoids and phenolic compounds. This extraction process is considered environmentally friendly as it utilizes water vapor as the solvent [2].

Steam distillation stages include; Preparation of raw materials that have been dried and chopped before being placed into the distillator. A steam vessel is connected separately, delivering hot steam that envelops the surface of the raw material. This steam causes the pores of the raw materials to open, stimulating the release of the oil fraction trapped within. The oil fraction, now released, diffuses with the water vapor and is carried to the cooled condenser, where it condenses into the liquid phase. The oil yield in steam distillation has been reported to be relatively low by previous researchers [3] [4] . To address this issue, some researchers have enhanced their methods, transitioning from super-hot steam distillation [5] to microwave-assisted distillation [6] which are claimed to be more effective in increasing oil yield.

In the essential oil refining industry, steam distillation is a well-established and commonly used method [7]. Increasing production without completely overhauling the method, which would involve acquiring new equipment, consuming additional energy, and preparing the workforce for technology transfer, is a key goal. The

challenge of achieving higher oil yields can often be traced back to the initial treatment of the raw materials. Prior to entering the distillation reactor, raw materials are typically dried to reduce moisture content and then chopped [8]. The chopping process essentially disrupts the tissue structure containing the oil sac, facilitating the oil fraction's diffusion with steam. However, because chopping occurs outside the reactor, some of the oil fraction may be lost prematurely. To prevent the loss of essential oils, the idea is to implement the chopping of raw materials directly within the distillation vessel. This approach ensures that the chopping process occurs simultaneously with the steam flow, resulting in more optimal capture of the oil fraction.

Our study delves into the intricate distillation procedures involved in extracting cempaka oil, a resource plentifully found in Sibang Village, within the Badung Regency of Bali [9]. Despite its abundance, this valuable commodity has remained largely untapped, with minimal processing into essential oil. Through our research, we aim to serve as a pivotal force propelling the development of the local refining industry. By distillation the potential of indigenous resources and unlocking their essence through advanced processing techniques, we pave the way for the conversion of these raw materials into lucrative, high-value products.

2. METHODS

2.1 Material

The test samples used in this study consisted of Champaca *(Magnolia champaca (L.) Figlar)* flowers harvested from Sibang Village, Badung Regency, Bali. Each experiment required 200 grams of orange Champaca flowers. To ensure consistency, all the flowers used were sourced from the same tree. To reduce humidity, all flowers were allowed to wilt in the sun. Subsequently, an electric oven was employed to evenly decrease moisture content throughout the Champaca flowers. The drying process was carried out at 60°C for 2 hours, a temperature chosen based on TGA results indicating that moisture reduction occurred effectively at temperatures below 61.68°C.

2.2 Experimental setup

The experiments using small-scale distillation equipment, comprising three main components: a distillator with a chopper module, a steam reactor, and a condenser. The distillation chamber measures 20x20x40 cm, the schematic is shown in Fig. 1.

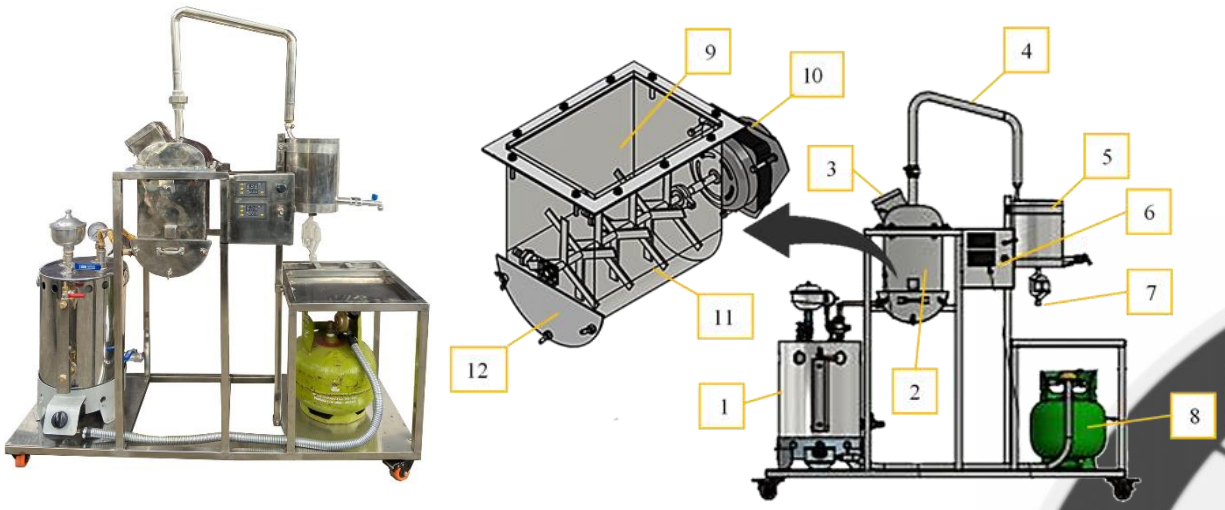

Figure 1. Experimental Setup; 1. Steam Reactor, 2. Distillation, 3. Material Input, 4. Steam Line, 5. Condenser, 6. Control, 7. Oil Output, 8. LPG, 9. Distillation Chamber, 10. Drive Motor, 11. Cutting Blade , 12. Residual output

2.3 Experimental Stage

This study examined the essential oil produced through steam distillation of Champaca flowers, considering three different treatment variations, as illustrated in the diagram, as shown in Fig. 2. The first experiment involved distillation of whole, unchopped Champaca flowers (X1), while the second experiment used Champaca flowers chopped within the distillation chamber (X2). The third experiment used Champaca flowers that were both chopped and dried before distillation (X3). All experiments maintained consistent control variables, including sample type, sample weight, distillation time, and sample size. The quantity of distilled Champaca oil was evaluated based on the percentage of the main component content determined by GC-MS analysis.

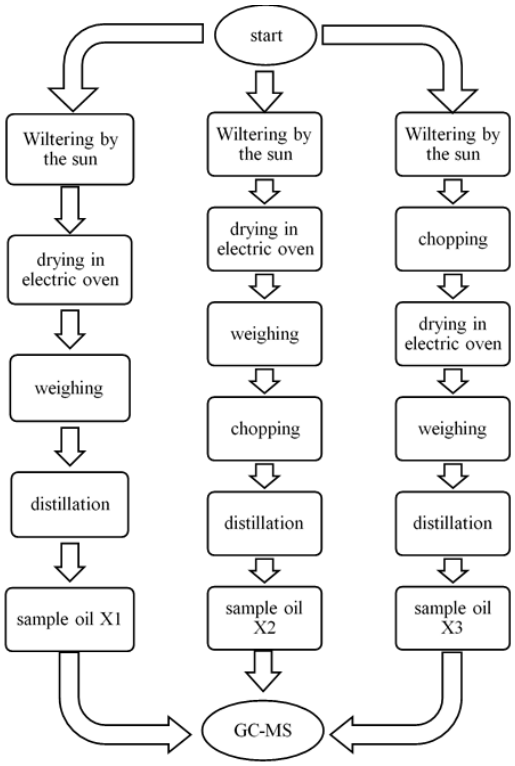

Figure 2. Experiment Stage

2.4 Thermogravimetric Analysis (TGA)

To investigate the biomass behavior under the influence of heat, we conducted a thermogravimetric analysis (TG/DTG) using the TGA-701 Leco instrument, with a measurement precision of ±2°C and a microbalance sensitivity of 0.0001 g. The test sample, comprising 1.0 g of Champaca flower. The sample was subjected to dynamic heating, ranging from room temperature to 950°C, with a heating rate of 20°C/min, all while maintaining a continuous flow of nitrogen gas at 10 mL/min.

2.5 Liquid Analysis

We analyzed the samples using a GC-MS system, which consisted of an Agilent 7890B chromatograph coupled with an Agilent 5977B-MSD spectrometer. The chromatography column employed was an HP-5 MS UI, and Helium served as the carrier gas with a sweep speed of 1.3 mL/min. The heating program was configured to initiate at 70°C for 3 minutes, followed by a ramping rate of 10°C/min until reaching 290°C, which was held for 2 minutes. Compound identification was automated through a comparison of mass spectra with the NIST-14 MS library. The MS scan range spanned from m/z 40 to 350, operating at a frequency of 4.5 scans per second. The gain factor was set at 1.0, and the Electron Multiplier (EM) was maintained at 1780 Volts. The MS source and quadrupole temperatures were set to 230°C and 150°C, respectively.

3. RESULTS AND DISCUSSION

3.1 Champaca Flower Characteristic

The characterization of Champaca flowers involved the microscopic observation of tissues using a Scanning Electron Microscope (SEM). The samples were split on the transverse side for testing, and the results

are presented in Fig. 3. The SEM images reveal that Champaca flower tissues contain pockets or cavities believed to house oil fractions. During the distillation process, steam's heat is employed to deform these tissues, widening them to facilitate the faster release and binding of oil fractions to steam. This process can be more effective if the path traveled by the oil is shorter, thus conserving energy. Shortening this path can be achieved by chopping raw materials before distillation. Therefore, we formulated a provisional hypothesis that chopping the material would lead to an increase in the oil yield.

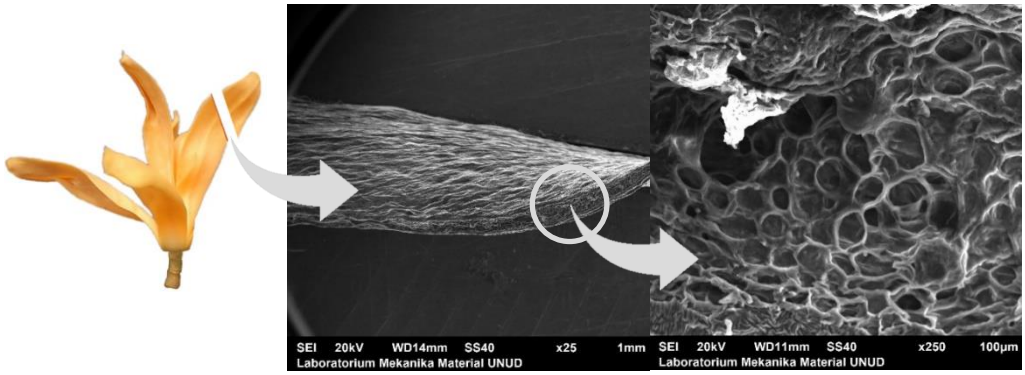

Figure 3. The Transverse Surface Of The Champaca Flower Viewed Using SEM At 25 And 250X Magnification

We conducted proximate analysis through TGA tests to analyze the decomposition process of Champaca flower biomass when subjected to heat. This analysis examines the decomposition of moisture, volatiles, fixed carbon, and ash at specific temperatures corresponding to the applied heat. The test results are presented in Table 1 and visualized in Fig. 4.

Table 1. Proximate Analysis of Champaca Flower

Parameters	%wt*
Moisture	85.41
Volatile (VM)	14.40
Fixed Carbon (FC)	0.13
Ash	0.05

**as received basis (sample was chopped)*

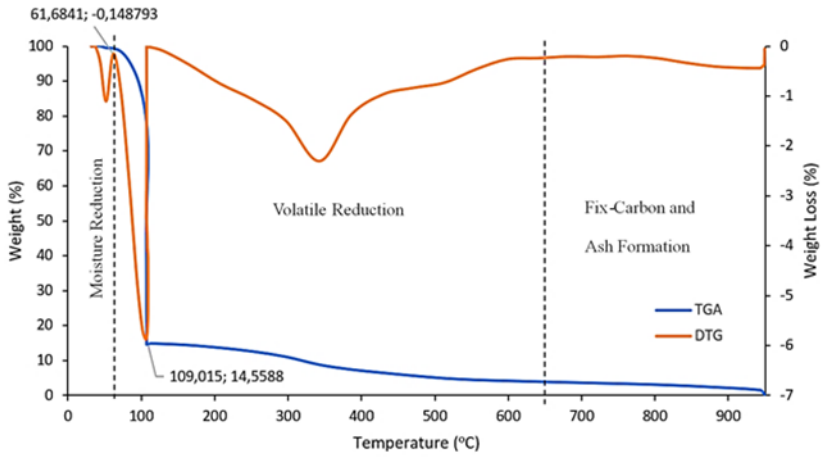

Figure 4. TGA-DTG diagram of Champaca flower

The TGA-DTG graph (Fig. 4) illustrates the reduction in sample mass with increasing heat, corresponding to rising temperatures. Initially, there is a rapid reduction in mass, reaching 85.41% at 109°C. This corresponds to

the moisture reduction phase, which typically occurs in the range of 100-110°C, leading to the evaporation of water present in the biomass [10]. Since essential oils have volatile properties, particularly those located outside the flower tissue structure, they are considered part of the water evaporation phase, leading TGA to categorize them as moisture reduction. The DTG graph exhibits a valley that ends at 61.68°C, indicating the initial stage of moisture reduction. To preserve essential oil content, it is advisable to conduct the initial drying stage at temperatures below 61°C, as supported by previous research [11]. The next sharp valley occurs until 109°C, representing a significant reduction in mass attributable to the loss of essential oils. Subsequently, there is a third valley within the temperature range of 109 to 650°C, indicating the evaporation of oil within the tissue structure, accounting for 14.4% of the overall oil content. Finally, there is a minimal mass reduction of 0.13% due to the loss of fixed carbon, leaving behind 0.05% as ash.

3.2 Analysis of Compounds in Distilled Champaca Oil

The distillation experiment yielded three oil samples, denoted as X1, X2, and X3, which were subsequently subjected to GC-MS (Gas Chromatography-Mass Spectrometry) analysis to determine their compound composition. The GC-MS test results are presented in two forms: spectral graphs and a list of compound types (Table 2). In Fig. 5, graph (a) illustrates 8 spectral peaks in sample X1, indicating the presence of 8 dominant types of compounds within this sample. Sample X2, shown in graph (b), exhibits 4 dominant spectra, signifying the presence of 4 dominant compound types. Meanwhile, sample X3, depicted in graph (c), displays 8 dominant spectra. The comparison of peak spectral height and retention time serves as the basis for identifying and categorizing compound types, referencing the NIST Chemistry Web-Book catalog [12].

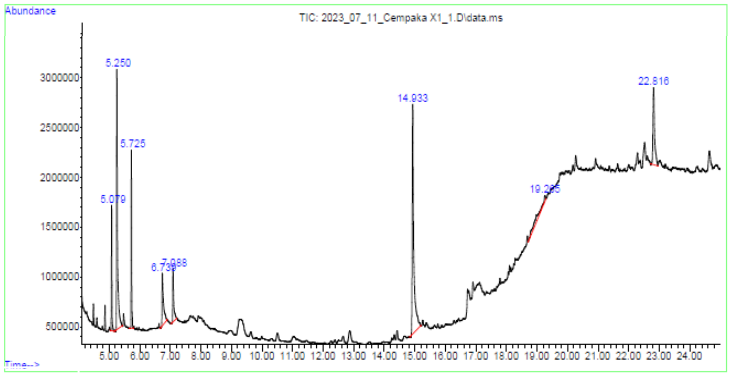

(a)

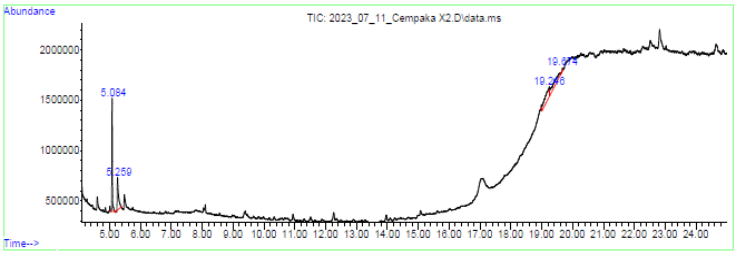

(b

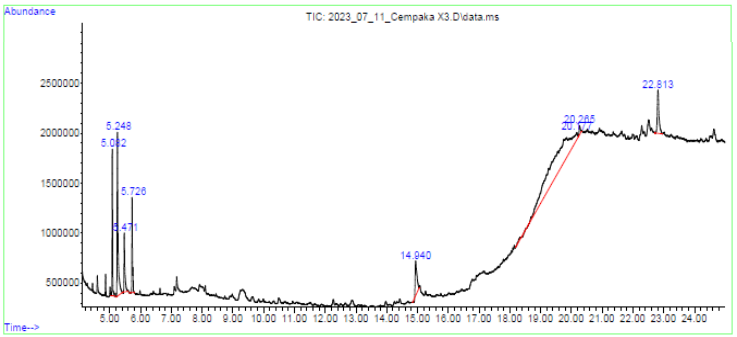

(c)

Figure 5. GC-MS Spectrum Graph: (a) X1, (b) X2 dan (c) X3

Linalool, a key component of essential oils, particularly Champaca oil, is represented by the molecular formula $C_{10}H_{18}O$ [13]–[15] with the molecular formula $C_{10}H_{18}O$. In this study, the quantity of Linalool was employed as an indicator to assess the distillation process's performance. Table 2 presents the column area section, showing the percentage of Linalool content in each sample. Sample X1 contains 6.54% Linalool, while sample X2 boasts the highest concentration at 32.33%, and sample X3 contains 7.4% Linalool. Notably, sample X2 exhibits the highest Linalool content, suggesting that the distillation process with internal chopping yields Champaca oil of superior quality compared to the other two methods.

Table 2. List Of Compounds in Champaca Oil Based On GC-MS Test Results

PK#	RT	Area%	Library/ID	Ref#	CAS#	Qual
			Sample : X1			
1	5.079	6.54	Linalool	27451	000078-70-6	91
2	5.250	22.85	Phenylethyl Alcohol	10108	000060-12-8	94
3	5.725	9.11	(3R,6S)-2,2,6-Trimethyl-6-vinyltetrahydro-2H-pyran-3ol	39780	039028-58-5	72
4	6.739	6.96	Indole	8731	000120-72-9	95
5	7.088	4.90	Methyl anthranilate	25546	000134-20-3	95
6	14.933	33.24	n-Hexadecanoic acid	117418	000057-10-3	99
7	19.265	4.49	Tetrasiloxane, decamethyl-	168283	000141-62-8	50
8	22.816	11.90	Acetic acid, [4-(1,1-dimethylethyl)phenoxy]-,methyl ester	85348	088530-52-3	47
			Sample : X2			
1	5.084	32.33	Linalool	27447	000078-70-6	96
2	5.259	20.66	Phenylethyl Alcohol	10107	000060-12-8	94
3	19.246	25.90	Tris(tert-butyldimethylsilyloxy)arsane	260810	1000366-57-5	52
4	19.674	21.12	Arsenous Acid, tris(trimethylsilyl) ester	199618	055429-29-3	52
			Sample : X3			
1	5.082	7.40	Linalool	27447	000078-70-6	96
2	5.248	14.31	Phenylethyl Alcohol	10108	000060-12-8	94
3	5.471	4.78	Benzyl nitrile	8741	000140-29-4	96
4	5.726	5.56	(3R,6S)-2,2,6-Trimethyl-6-vinyltetrahydro-2H-pyran-3ol	39780	039028-58-5	83
5	14.940	5.38	n-Hexadecanoic acid	117419	000057-10-3	97
6	20.177	54.72	2" -Hydroxy-5' -methylacetophenone, TMS derivative	85149	97389-69-0	50
7	20.265	1.02	2,4,6-cycloheptatrien-1-one,3,5-bis-trimethylsilyl-	111265	1000161-21-8	50
8	22.813	6.83	1,2-Bis(trimethylsilyl)benzena	85160	017151-09-6	50

The distillation of whole Champaca flowers yields the lowest Linalool content and also includes seven other types of compounds, such as acids (45.14% - including n-Hexadecanoic acid and Acetic acid), alcohols (22.85%), and aromatic hydrocarbon compounds (25.46% - including Trimethyl, Indole, Methyl anthranilate, and Tetrasiloxane). The presence of these additional compounds is attributed to the excess heat absorbed by the flower tissues during distillation. This occurs when the trapped oil has to traverse a lengthy trajectory, causing it to decompose due to the heat into various other compounds. High temperatures promote chemical reactions between compounds, leading to the formation of new compounds. A similar pattern is observed in sample X3, where the distillation process initiates with the drying of chopped samples, causing the rapid evaporation of Linalool, leaving only a minimal amount. Elevated temperatures further promote the decomposition of tissue components into hydrocarbon compounds, constituting 72.91% of the total composition. These hydrocarbon compounds include Benzyl nitrile, Trimethyl, methylacetophenone, cycloheptatrien, and benzena. Additionally, alcohol compounds make up 14.31% of the composition, followed by acids at 5.38%. The distillation process using the internal chopping method effectively retains Linalool components within the tissue pockets. When exposed to steam, these components readily escape and diffuse with the steam, as illustrated in Fig. 6. Because Linalool compounds are positioned internally, they can flow shorter distances. It can be inferred that smaller cutting sizes result in higher

Linalool compound content in the oil. This observation aligns with findings from previous researchers [16], [17], although they employed external chopping methods before the distillation process.

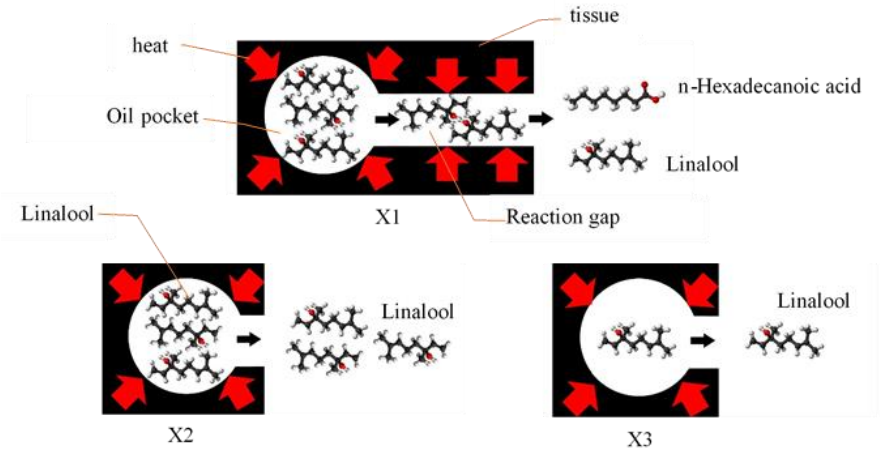

Figure 6. Reaction scheme and release of compounds in tissues

In addition to Linalool, the internal enumeration method yields alcohol compounds (Phenylethyl Alcohol) at a concentration of 20.66% and acids at 47.02% (including arsane and Arsenous Acid). Both of these compound groups are formed due to the presence of excess oxygen, particularly in the steam containing oxygen. Notably, compared to the other two methods, the internal chopping method produces only three additional types of compounds aside from Linalool. This suggests that the subsequent purification process will be more straightforward and efficient.

4. CONCLUSION

Linalool emerges as the predominant compound in champaca oil obtained through steam distillation. Varied chopping methods employed during the distillation process result in differing concentrations of Linalool compounds. Specifically, unchopped essential materials yield Linalool compounds at a rate of 6.54%, internal chopping produces 32.33%, and external chopping yields 7.40% Linalool compounds. The volatile nature of essential oils underscores the necessity for precise distillation techniques. The internal chopping method notably yields the highest concentration of Linalool compounds. Hence, it can be inferred that incorporating internal chopping of materials within the distillation reactor effectively enhances the main compound content during steam distillation processes.

5. ACKNOWLEDGEMENT

This research was funded by Politeknik Negeri Bali, based on contract No. 1733/PL8/AL.04/2023, year 2023.

6. REFERENCES

[1] H. S. Kusuma and M. Mahfud, “The extraction of essential oils from patchouli leaves (Pogostemon cablin benth) using a microwave air-hydrodistillation method as a new green technique,” *RSC Adv.*, vol. 7, no. 3, pp. 1336–1347, 2017, doi: 10.1039/c6ra25894h.

[2] C. A. Machado, F. O. Oliveira, M. A. de Andrade, K. V. S. Hodel, H. Lepikson, and B. A. S. Machado, “Steam Distillation for Essential Oil Extraction: An Evaluation of Technological Advances Based on an Analysis of Patent Documents,” *Sustain.*, vol. 14, no. 12, 2022, doi: 10.3390/su14127119.

[3] H. Zhang *et al.*, “Extraction of Camphor Tree Essential Oil by Steam Distillation and Supercritical CO2 Extraction,” *Molecules*, vol. 27, no. 17, 2022, doi: 10.3390/molecules27175385.

[4] K. Řebíčková, T. Bajer, D. Šilha, K. Ventura, and P. Bajerová, “Comparison of Chemical Composition and Biological Properties of Essential Oils Obtained by Hydrodistillation and Steam Distillation of Laurus nobilis L.,” *Plant Foods Hum. Nutr.*, vol. 75, no. 4, 2020, doi: 10.1007/s11130-020-00834-y.

[5] M. A. Ayub, G. Goksen, A. Fatima, M. Zubair, M. A. Abid, and M. Starowicz, “Comparison of Conventional Extraction Techniques with Superheated Steam Distillation on Chemical Characterization and Biological Activities of Syzygium aromaticum L. Essential Oil,” *Separations*, vol. 10, no. 1, 2023, doi: 10.3390/separations10010027.

[6] K. Beyecha Hundie, T. Aga Bullo, Y. Mekonnen Bayisa, D. Abdissa Akuma, and M. Seid Bultum,

"Optimization of microwave-assisted hydro-distillation essential oil extracted from Rumex Crispus leaves using definitive screening design," *Arab. J. Chem.*, vol. 16, no. 5, 2023, doi: 10.1016/j.arabjc.2023.104665.

[7] W. Rinaldi *et al.*, "Development of a unique method to evaluate the effectiveness of traditional steam distillation of patchouli essential oil," *Mater. Today Proc.*, vol. 63, 2022, doi: 10.1016/j.matpr.2021.12.406.

[8] S. K. Pandey, N. Sarma, T. Begum, and M. Lal, "Standardization of Different Drying Methods of Fresh Patchouli (Pogostemon cablin) Leaves for High Essential Oil Yield and Quality," *J. Essent. Oil-Bearing Plants*, 2020, doi: 10.1080/0972060X.2020.1798289.

[9] D. Ka. Badung, "Pembinaan Teknologi Tepat Guna di Desa Sibangkaja Tahun 2023." https://dpmd.badungkab.go.id/berita/51637-pembinaan-teknologi-tepat-guna-di-desa-sibangkaja-tahun-2023

[10] Z. Guo, C. Li, L. Wang, G. Wang, Z. Wang, and D. Wang, "EFFECTS OF TRIPLE-PASS DRUM DRYER ON ENZYME ACTIVITY AND QUALITY OF FORAGE OATS," *Appl. Eng. Agric.*, vol. 38, no. 4, 2022, doi: 10.13031/aea.14962.

[11] B. C. O'Kelly and V. Sivakumar, "Water Content Determinations for Peat and Other Organic Soils Using the Oven-Drying Method," *Dry. Technol.*, vol. 32, no. 6, 2014, doi: 10.1080/07373937.2013.849728.

[12] T. N. I. of S. and T. (NIST), "NIST Chemistry WebBook, SRD 69." [Online]. Available: https://webbook.nist.gov/

[13] K. Pokajewicz, M. Białoń, L. Svydenko, R. Fedin, and N. Hudz, "Chemical composition of the essential oil of the new cultivars of lavandula angustifolia mill. Bred in ukraine," *Molecules*, vol. 26, no. 18, 2021, doi: 10.3390/molecules26185681.

[14] S. Dhandapani, J. Jin, V. Sridhar, R. Sarojam, N. H. Chua, and I. C. Jang, "Integrated metabolome and transcriptome analysis of Magnolia champaca identifies biosynthetic pathways for floral volatile organic compounds," *BMC Genomics*, vol. 18, no. 1, 2017, doi: 10.1186/s12864-017-3846-8.

[15] H. T. Chang, C. Y. Lin, L. S. Hsu, and S. T. Chang, "Thermal degradation of linalool-chemotype cinnamomum osmophloeum leaf essential oil and its stabilization by microencapsulation with β-cyclodextrin," *Molecules*, vol. 26, no. 2, 2021, doi: 10.3390/molecules26020409.

[16] A. M. Gumelar, E. Ersan, and D. Supriyatdi, "Pengaruh Lama Pelayuan dan Pencacahan Daun Serai Wangi (Cymbopogon winterianus Jowitt ex Bor) pada Rendemen dan Mutu Citronella Oil," *J. Agro Ind. Perkeb.*, 2022, doi: 10.25181/jaip.v10i1.1644.

[17] G. M. Sabila, C. Sephia, T. Karliati, Y. Suhaya, and R. Dungani, "Washing and Chopping Pre-treatment Effect of Vetiver Roots on Vetiver Oil Yield and Distillation Time," in *IOP Conference Series: Earth and Environmental Science*, 2021, vol. 891, no. 1. doi: 10.1088/1755-1315/891/1/012021.